DOE/MC/21181-1950, Vol. 14
(DE90000451)

Geological Evolution and Analysis of Confirmed or Suspected Gas Hydrate Localities

Volume 14. Basin Analysis, Formation and Stability of Gas Hydrates of the Timor Trough

Topical Report

P.D. Finley
J. Krason

Work Performed Under Contract No.: DE-AC21-84MC21181

For
U.S. Department of Energy
Office of Fossil Energy
Morgantown Energy Technology Center
P.O. Box 880
Morgantown, West Virginia 26507-0880

By
Geoexplorers International, Inc.
5701 East Evans Avenue
Denver, Colorado 80222

October 1989

PREFACE

This document is Volume XIV of a series of reports entitled *Geological Evolution and Analysis of Confirmed or Suspected Gas Hydrate Localities.* Volume XII is a study titled *Basin Analysis, Formation and Stability of Gas Hydrates of the Timor Trough.* This report presents a geological description of the subduction zone between the northwest margin of Australia and Indonesia, including regional and local structural settings, geomorphology, geological history, stratigraphy, and physical properties. It provides the necessary regional geological background for more in-depth research of the area. Detailed discussion of bottom simulating acoustic reflectors, sediment acoustic properties, and distribution of hydrates within the sediments are also included in this report. The formation and stabilization of gas hydrates in sediments are considered in terms of phase relations, nucleation, and crystallization constraints, gas solubility, pore fluid chemistry, inorganic diagenesis, and sediment organic content. Together with a depositional analysis of the area, this report is a better understanding of the thermal evolution of the locality. It should lead to an assessment of the potential for both biogenic and thermogenic hydrocarbon generation.

Project Manager
Gas Hydrates

CONTENTS

CONTENTS

(continued)

ILLUSTRATIONS

TABLES

BASIN ANALYSIS, FORMATION AND STABILITY OF GAS HYDRATES OF THE TIMOR TROUGH

By Patrick Finley and Jan Krason

EXECUTIVE SUMMARY

Geological factors controlling the formation, stability, and distribution of gas hydrates in the Timor Trough region were investigated by basin analysis. Geological, geophysical, and geochemical data from the region were assembled and evaluated to determine the relationships of geological environments and gas hydrates.

This study was performed for the U.S. Department of Energy, Morgantown Energy Technology Center by Geoexplorers International, Inc. as part of an evaluation of 21 offshore sites worldwide where the presence of gas hydrates has been confirmed or inferred.

The Timor Trough is located between the Indonesian island of Timor and the northwest margin of Australia . The floor of the Timor Trough is 1,800 m to 3,400 m deep and ranges in width from 3 to 20 km. The trough extends for about 600 km. The Timor Trough is part of the Banda Arc system; it is bounded to the west by the Java Trench and the Aru Basin to the east.

The Timor Trough is generally interpreted as a collision zone between the Australia-India Plate and the Eurasia Plate. Continental crust of the Australian craton is being subducted beneath oceanic crust at the Timor Trough. The accretionary prism has formed on the inner (north) flank of the Timor Trough.

The outer slope of the Timor Trough consists of over 5 km of marine sediments deposited on Precambrian continental crust of Australia. The strata of the outer slope of the Timor Trough can be divided into four seismic units. The lowermost unit was deposited in the Paleozoic in intracratonic basins. The second sequence is composed of Upper Permian to Middle Jurassic clastic deposits. These rocks were deposited in rifts produced during the formation of the passive margin of Australia by continental breakup. The syn-rifting rocks were uplifted and eroded in the final stages of continental breakup, producing a regional unconformity. The third sequence is composed of continental margin sediments deposited on the passive margin produced by the middle Jurassic continental breakup. The sequence grades upward from hemipelagic shales and

carbonates to shelf carbonates. This sequence averages 1.5 km thick in the southeastern segment of the Timor Trough. The unit records the deposition and building of the continental slope and continental shelf of Australia from the Early Cretaceous to late Tertiary time. The fourth stratigraphic sequence of the outer slope of the trough was deposited in progressively deeper water. The sediments grade upward from shelf carbonates to hemipelagic carbonate oozes representing the deflection of the Australian margin into the Timor Trough after the onset of subduction. The sequence averages 250 m, but varies in thickness and continuity between seismic lines.

The outer slope of the Timor Trough is cut by numerous faults. Normal faults in the southeastern portion of the Timor Trough decrease in displacement upward, indicating reactivation of ancestral faults as the slope began the flexure and descent into the trough. Reverse faults predominate in the outer slope of the northeastern portion of the trough.

The floor of the Timor Trough is filled by a wedge of horizontally stratified mass-wasting deposits. The trough floor varies in width from less than 1 km to 17 km. The irregularity of the trough floor morphology is due to folding and thrusting of underlying sediments in response to compressional forces.

The inner (north) slope to the trough is composed of upper slope and lower slope sections. The upper slope is generally marked by a relatively smooth sea floor, the slope of which gradually increases with water depth. Except for a thin surface veneer of sediments, no seismic reflectors can be resolved from within the upper slope areas. The lower-slope section extends from a seafloor depth of about 1,500 m to the trough floor, and consists of large folds and thrust sheets. The folds serve to dam downslope sediment transport and form small slope basins. The two distinct slope types reflect contrasts in the material being accreted. The lack of coherent internal reflections in sediments of the upper slope indicates that the sediments are clay-rich and have been subjected to small-scale deformation. The sediments composing the upper slope are trough fill and surficial hemipelagic sediments originally deposited on the continental rise of Australia. The large thrust sheets of the lower slope which retain seismic coherence at depth consist of more competent material, principally indurated continental shelf and slope lithologies. Since the accreted material of the lower slope is more thoroughly indurated, it failed along large thrust systems, rather than by internal shear and small-scale deformation as for the upper slope.

The floor of the Timor Trough was cored during Leg 27 of the Deep Sea Drilling Project. Site 262 was located near the southwest end of the trench at a water depth of 2,300 m. A 442 m sediment section of Holocene to Pliocene age was recovered. A well-lithified calcarenite at the base of the hole and an overlying dolomitic mud totalling 31 m were deposited under very shallow water in a continental shelf environment. A 76 m section of thick nannofossiliferous ooze records very rapid deepening of the sea in late Pliocene time. Overlying Pleistocene and Holocene units were deposited beneath water depths very similar to present depths. The sediments contain an average of 0.8% total organic carbon. Cores recovered from subbottom depths of 5 m to the bottom of the hole released biogenic methane gas.

Geochemical data from DSDP Site 262 suggests that evaporates underlie the Timor Trough. Organic geochemical analyses indicate that Pleistocene to

Holocene sediments contain more organic carbon than underlying sediments, and that the organic matter is more gas-prone. The sediments of the Timor Trough are adequate sources for biogenic methane, but are generally immature with respect to generation of thermal hydrocarbons. However, sediments of the outer slope are heated as they are subducted into the trough. The subducted sediments and sediments of the inner slope which have been deeply buried by imbricate thrust faulting may be generating thermogenic hydrocarbons.

The Timor Trough study region was included in this study of gas hydrate locations based on the geochemistry of cores recovered from DSDP Site 262. No hydrates were recovered from sediments at DSDP Site 262. Gas emission from the recovered cores increased the core volume by about 25%. However, simple exsolution methane dissolved in pore water could account for a similar degree of core expansion without hydrates being present.

Gas hydrates were proposed to exist at DSDP Site 262 to rectify an apparent paradox in pore water geochemical data from Site 262. High alkalinity values for the upper 250 m of the hole indicated active bacterial degradation of organic carbon to carbon dioxide. The salinity of the pore water increased rapidly to the bottom of the hole, reaching 54 ppt at 441 m subbottom, presumably indicating diffusion from an underlying evaporate bed. McKirdy and Cook (1980) proposed that the alkalinity peak in the pore water geochemical profile of Site 262 was a relict feature which indicated past levels of bacterial activity. However, diffusion of pore-water constituents evidenced by the increase of salinity with depth would be expected to have obliterated any such relict alkalinity enrichment. McKirdy and Cook (1980) proposed that gas hydrate in the sediment section at Site 262 "reduces the effective permeability to zero, thus blocking fluid migration in the top 300 m of the section." They postulated the presence of gas hydrates to reconcile the observed diffusion-controlled salinity profile below 300 m subbottom depth and a relict alkalinity peak in the shallower sediments.

We do not interpret the geochemistry of the pore water at DSDP Site 262 to indicate hydrate presence. The alkalinity curve from Site 262 is not anomalous; it is a result of normal bacterial action on organic matter in marine sediments. Gas hydrate presence is not required to explain the alkalinity variation down-hole.

No seismic evidence of gas hydrates in sediments of the Timor Trough has been reported in the literature. Our review of seismic lines from the study region has detected bottom simulating reflectors (BSRs) on various seismic lines from the north flank of the Timor Trough. In addition to discordance of the BSRs and sediment reflectors, a possible velocity anomaly exists above some of the reflectors.

With no confirmed evidence of hydrates in the Timor Trough study region potential gas estimates are speculative. Bottom simulating reflectors were detected along an area of the accretionary prism offshore of western Timor measuring about 5,000 km^2. We project that about 20% of the area is indeed underlain by BSRs, for a net areal extent of 1,000 km^2. Assuming that the impedance contrast that causes the BSRs is due to hydrate filling 50% of the pore space of a 40% porosity sediment, a 1 m thick layer of hydrate-impregnated sediment would contain 2×10^8 m^3 of hydrate. Using a volumetric conversion

factor of 150 m^3 gas per m^3 hydrate, about 3×10^{10} m^3 or 1 trillion cubic feet (tcf) may be present as hydrates. A 10 m thick layer of 40% porosity sediment with 50% of the pore space filled with hydrate would contain 3×10^{11} m^3 or 10 tcf of gas.

The BSRs of the Timor Trough study region often correspond to anticlines with a bathymetric expression. This mode of occurrence is conducive to trapping free gas beneath the hydrate layer. Bathymetric highs on the accretionary prism offshore of Timor are capable of containing about 10^{10} m^3 or 0.3 tcf of gas in sub-hydrate traps. There is no evidence as to whether any of the potential sub-hydrate gas traps presently contain any reservoired gas.

INTRODUCTION

Gas hydrates are solid substances composed of small gas molecules enclosed in a crystal lattice of water molecules. Gas hydrates can be formed from various gases and water at high pressures and low temperatures when a sufficiently high concentration of dissolved gas exists. Conditions favorable for natural gas hydrate formation and preservation occur in some continental margin and deep sea sediments where adequate amounts of hydrocarbon gases are available. Large quantities of natural gas with possible resource potential may be present in offshore gas hydrates or trapped beneath impermeable gas hydrate layers.

This report presents the results of a study on the geological factors which control the formation and stability of gas hydrates in the sediments of the Timor Trough. The Timor Trough study region is located in the Indian Ocean between the northwest continental shelf of Australia and the Indonesian island of Timor. This study is part of a project performed for the U.S. Department of Energy's Morgantown Energy Technology Center by Geoexplorers International, Inc. The main purpose of the project is to evaluate the geological controls of gas hydrate formation and stability and to make preliminary assessments of gas resources associated with gas hydrates.

Gas hydrates were originally proposed to exist in the Timor Trough study based on geochemical anomalies in cores recovered from the floor of the trough. Abundant methane gas occurs in the cores. No direct evidence of gas hydrates in the study region has been reported in the literature. No examples of seismic evidence of gas hydrates in the Timor Trough have been identified in the literature.

In this study we have assembled and analyzed all available information of gas hydrates in the Timor Trough study region. We document new seismic evidence of gas hydrate presence in the region and assess its relationship to geological factors. We discuss and assess data which suggest that gas hydrates exist in sediments of the Timor Trough.

This report is presented in two sections:

Part I - Basin Analysis examines the structural geology and sedimentary environments of the Timor Trough study region. Based on this information, the regional hydrocarbon generation potential is discussed.

Part II - Formation and Stability of Gas Hydrates describes the seismic and drilling evidence of gas hydrate presence in the study region. The evidence is analyzed in detail in view of the information presented in Part I to indicate which factors may control the formation and stability of gas hydrates in the Timor Trough study region.

Acknowledgements

Geoexplorers International, Inc. and the authors are grateful to the U.S. Department of Energy, Morgantown Energy Technology Center for the opportunity to participate in the gas hydrate research program. Rodney Malone of METC reviewed the report for technical content and style. Charles Komar expedited printing of this report.

PART I

BASIN ANALYSIS

The Timor Trough is located north of Australia, between the northwest margin of Australia and the Indonesian island of Timor. The crust of the Australian continent is being subducted beneath the oceanic crust underlying Indonesia at the Timor Trough. The subduction has produced a thick accretionary prism of sediments scraped from the descending plate. The sediments from the floor of the Timor Trough include carbonate trench-fill turbidites, and carbonate sediments deposited on the northern margin of the Australian continent in continental rise, slope, and shelf environments. The sediments drilled in the Timor Trough have adequate organic carbon for biogenic methane formation. Burial depths in basins in the subducting plate, and within the accretionary prism offshore of Timor may be sufficient for thermogenic hydrocarbon generation.

Location

The Timor Trough is located between the Indonesian island of Timor and the northwest margin of Australia (Figure 1). The Timor Trough has a flat floor 1,800 m to 3,400 m deep and ranges in width from 3 to 20 km. The trough extends for about 6,000 km. The Timor Trough is part of the Banda Arc system; it is bounded to the west by the Java Trench and the Aru Basin to the east.

Tectonics

The Timor Trough is generally interpreted as a collision zone between the Australia-India Plate and the Eurasia Plate. Continental crust of the Australian craton is being subducted beneath oceanic crust at the Timor Trough. The accretionary prism has formed on the inner (north) flank of the Timor Trough. The complex geology of Timor provides information on the timing and extent of deformation resulting from the plate collision.

Regional

The Timor Trough is a segment of the Banda Arc (Figure 2). The arc is a presently active subduction system. The Banda Arc and the Sunda Arc to the northwest constitute the Indonesian subduction system (Hamilton, 1979). The Banda Arc and the Sunda Arc have well-defined parallel structures typical of sub-

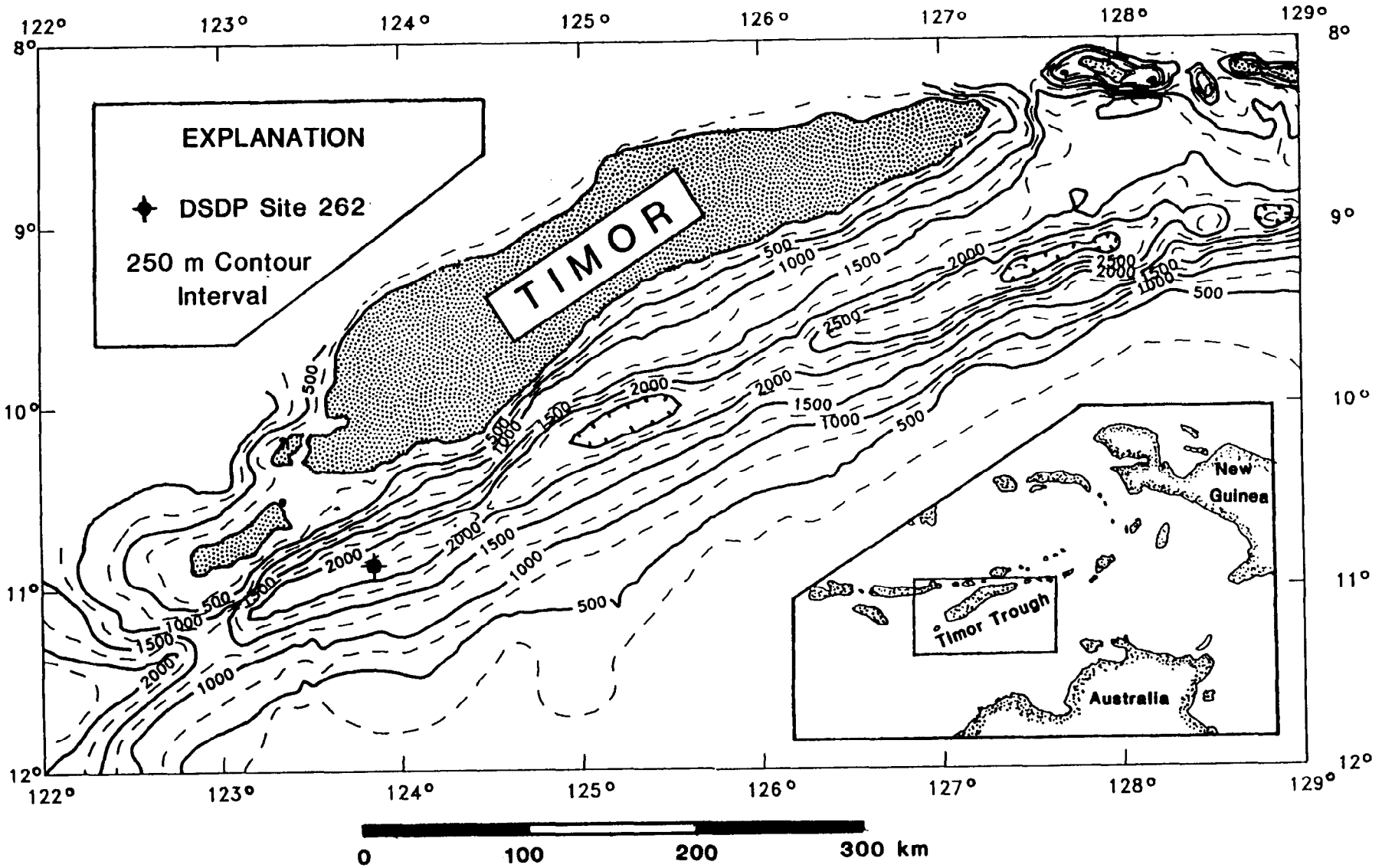

Figure 1. LOCATION AND BATHYMETRY OF THE TIMOR TROUGH

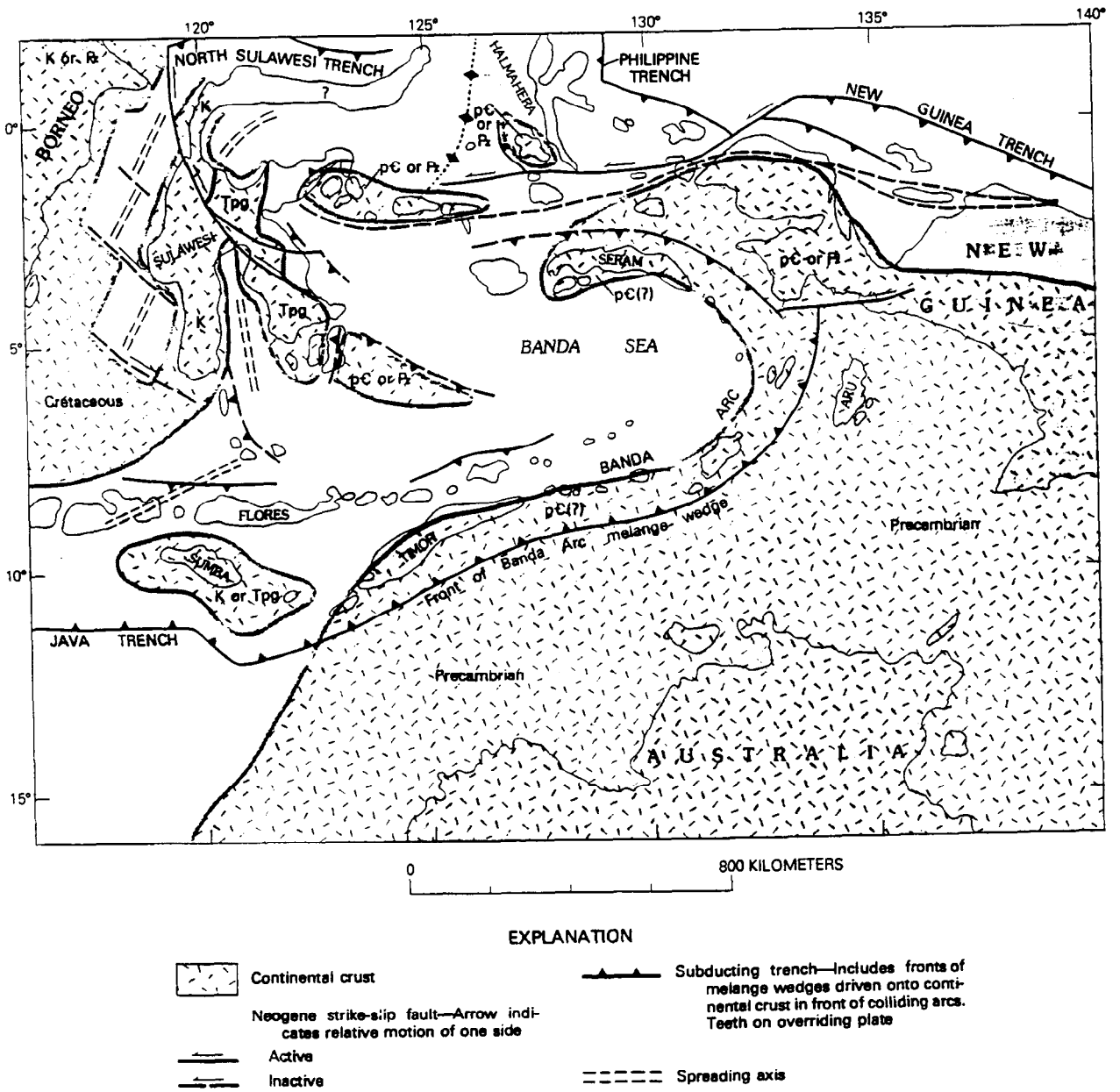

Figure 2. **TECTONIC FEATURES OF EASTERN INDONESIA**

From Hamilton, 1979

duction systems: trench, accretionary prism, forearc basin and inner volcanic arc. From the northwest, the Indonesian subduction system is made up of the Java Trench, where the oceanic crust beneath the Indian Ocean is being subducted beneath the Cretaceous continental crust of northern Indonesia and southeast Asia. The Sunda Arc traces a gentle curve along the 7,000 km Java trench; the trend of the subduction system changes from due south at the northern terminus of the Java Trench to east-southeast where the trench shallows offshore of Sunda. The subduction system bends sharply southwest end of the Timor Trough, which constitutes the beginning of the Banda Arc. The Banda Arc assumes an east-northeast trend through the Timor Trough and the Aru basin, as a consequence of the collision with the Australian continent (Charlton, 1989; Hamilton, 1979). In the Seram Trough, west of New Guinea, the Banda Arc rotates sharply to the north, northwest and eventually due west, in response to westward translation of the northern portion of New Guinea (Irian Jaya).

An accretionary prism is developed northeast of the trench-trough system of the Sunda Arc. Through most of the length of the Java Trench, the accretionary prism is not emergent, but is expressed as a submarine ridge. The the relief between the The floor of the Java Trench and the ridge ranges from 500 to 3,000 m.

A larger accretionary prism has been developed in conjunction with the subduction of the Australian continental crust along the Banda Arc. Sediments deposited on the continental shelf and slope of the northwestern margin of Australia have been offscraped as the Australian plate is subducted along the Timor Trough segment of the Banda Arc. The continental sediment input, along with possible uplift due to subduction of more buoyant continental crust, has produced an voluminous accretionary prism which has been uplifted above sea level. The island chain consisting of Savu, Roti, Timor, and the Tannibar Islands is principally composed of the uplifted accretionary prism produced from subduction of the Australian continental crust. Similarly, the islands of Seram and Buru have been formed and uplifted as a result of accretion by offscraping during subduction along the Seram Trough.

Well-defined forearc basins parallel the accretionary prisms of the Banda Arc. North of Timor, a synclinal depression extends from the Savu Basin northeastward through the Wetar Strait to the Weber basin north of the Tannimbar Islands.

A volcanic arc of the Sunda Arc includes of a large chain of islands including Sumatra, Java, Bali, and Lambak associated with the Java Trench. The Flores Islands, Alor, Wetar, and a chain of much smaller volcanic islands to the east mark the volcanic arc produced from subduction along the Timor Trough.

Timor Trough

While the region near Timor had been widely recognized as the locus of the collision between the Eurasia Plate and the India-Australia Plate, the site of the subduction has been debated. Seismic lines from the Timor Trough indicate that thrusting is occurring at the base the north slope of the trough. The imbricate thrust sheets which compose the shelf and slope south of Timor are consistent with subduction occurring at the floor of the trough (Figure 2). However, an alternative interpretation by Milson and Audley-Charles (1986) and Park (1987)

assigns a minor role to the thrust faulting occurring in the Timor Trough. As diagrammed by Park (1987), a complicated situation was proposed whereby the surface expression of the plate collision is in the shallow basin beneath the Wetar Strait (Figure 3). By the model of Milson and Audley-Charles (1986) and Park (1987), the Australian continental crust is not being subducted, but is overriding the oceanic crust of the Eurasian Plate. The thrusting in the Timor Trough is projected by Milson and Audley-Charles (1986) and Park (1987) to be minor intraplate adjustment in the overriding thrust sheet composed of Australian continental crust (Figure 3). However, most workers have preferred to interpret the subduction front to be located at the floor of the Timor Trough (e.g. Beck and Lehner, 1974; Bowin et al., 1980; Hamilton, 1979, Veevers, 1974a, 1974b, 1982, and Veevers and Heirtzler, 1974)

Seismic profiling and side-scan sonar images by Karig et al. (1987) definitively show that subduction is occurring along the foot of the inner slope of the Timor Trough (Figure 4). Karig et al. (1987) conducted a detailed survey of a short segment of the Timor Trough between 123.5° and 124.4°, and a corresponding area of the Savu Basin north of Timor. The northwestern continental margin of Australia is being subducted beneath Timor. Large thrust sheets composed of continental shelf and slope sediments are being scraped from the descending plate and accreted to the sedimentary prism of which Timor is a part. In contrast, the forearc basin north of Timor shows little evidence of compressional deformation.

The work reported by Karig et al. (1987) presents the most comprehensive description and discussion of the tectonics of the Timor Trough available in the literature. While their work concentrated on a small area offshore of the far western part of Timor, their interpretation can be confidently extended to other portions of the study region. The following synopsis of the structure and tectonics of the Timor Trough study region is drawn largely from Karig et al. (1987), with additional information from Montecchi (1976), Hamilton (1979) and Charlton (1989).

Outer Slope. The outer slope of the Timor Trough consists of over 5 km of marine sediments deposited on Precambrian continental crust of Australia. Karig et al. (1987) divided the strata of the outer slope of the Timor Trough into four seismic units (Figure 5). The lowermost unit was deposited in the Paleozoic in intracratonic basins. While evidence of this Paleozoic unit abounds from onland Australia and from the Australian continental shelf, Karig et al. (1987) found little evidence of these strata in the Timor Trough region. The second sequence is composed of Upper Permian to Middle Jurassic clastic deposits. These rocks were deposited in rifts produced during formation passive margin by continental breakup. The syn-rifting rocks were uplifted and eroded in the final stages of continental breakup, producing a regional unconformity. The two basal units were combined by Karig et al. (1987) for seismic interpretation. In Figure 5, the pre- and syn-rift sediments are indicated by the letter "A" and the breakup unconformity by "D".

The third sequence defined by Karig et al. (1987) is composed of continental margin sediments deposited on the passive margin produced by the middle

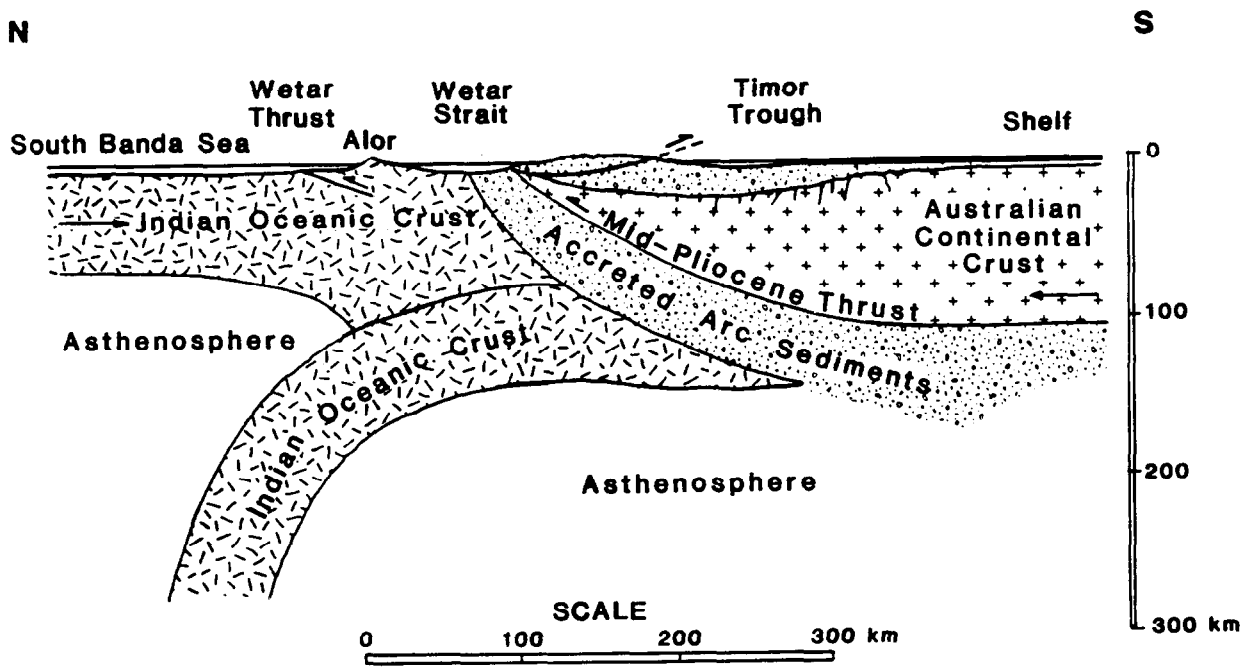

Figure 3. INTERPRETIVE CROSS SECTION OF STUDY REGION SHOWING PLATE BOUNDARY NORTH OF TIMOR

After Park, 1987

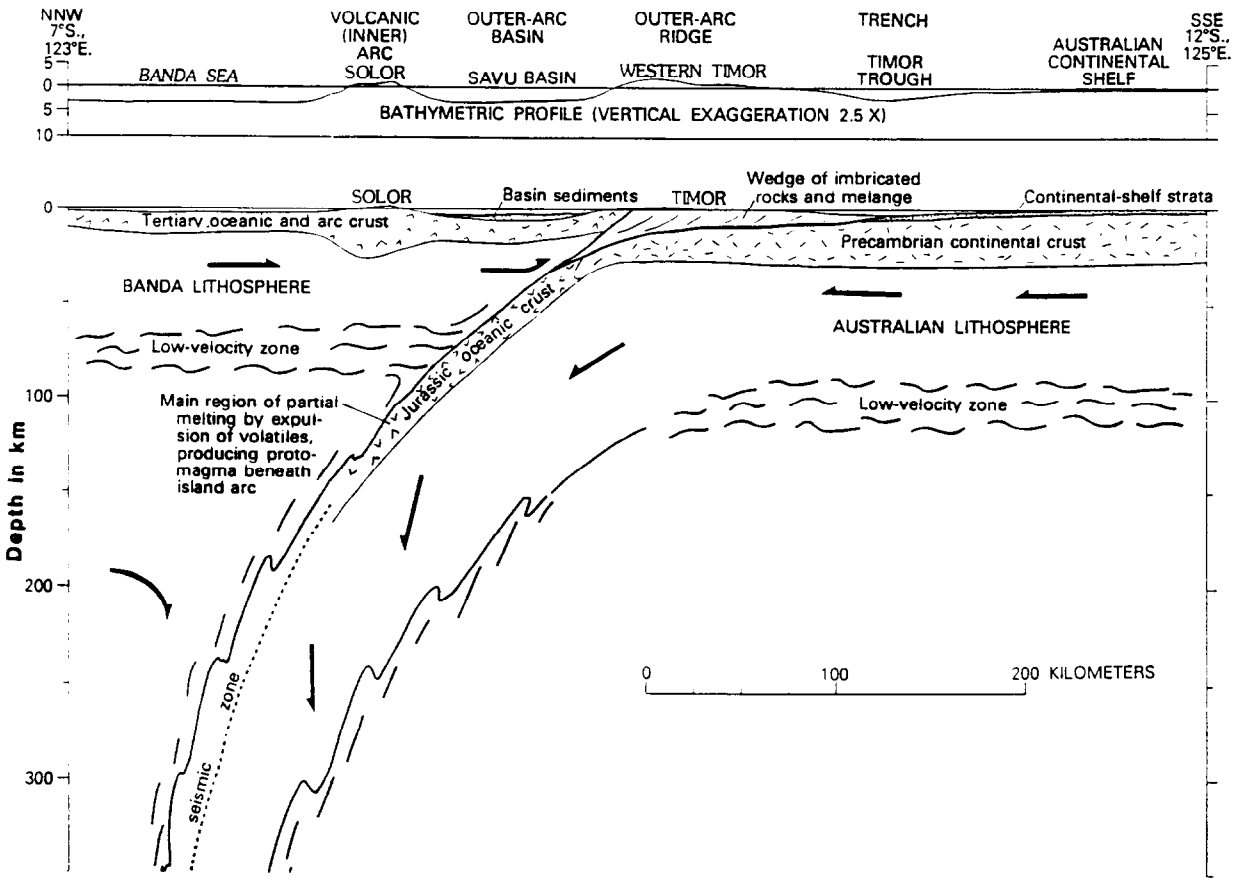

Figure 4.

INTERPRETIVE CROSS SECTION OF STUDY REGION SHOWING PLATE BOUNDARY AT THE FLOOR OF THE TIMOR TROUGH

From Hamilton, 1979

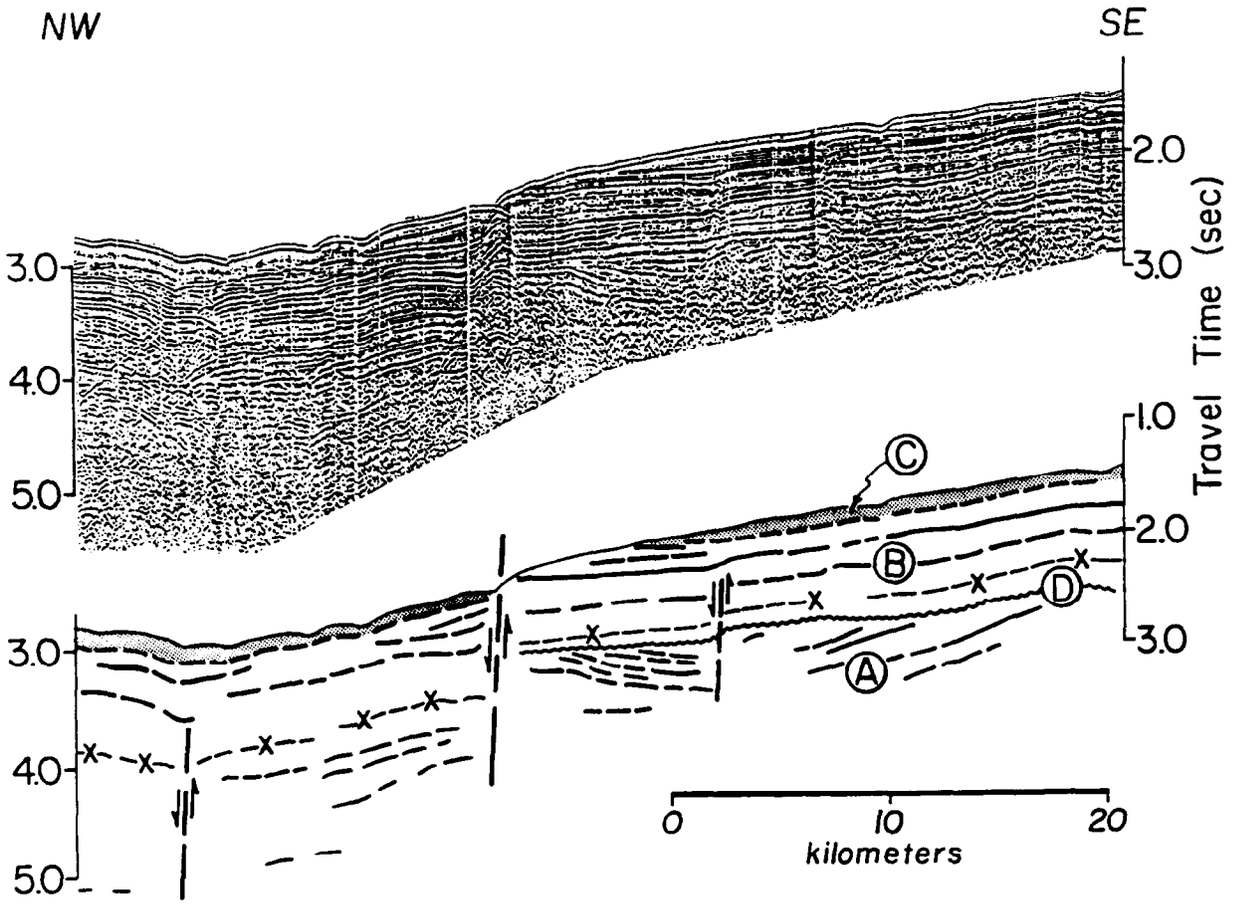

Figure 5. SEISMIC PROFILE 246, OUTER SLOPE OF THE TIMOR TROUGH

Seismic stratigraphy units: (A) Pre-rift strata, (B) Passive margin strata, (C) Outer slope strata, (D) Breakup unconformity.

From Karig et al., 1987

Jurassic continental breakup. The sequence grades upward from hemipelagic carbonates and shales to shelf carbonates. This sequence, indicated by the letter "B" in Figure 5 averages 1.5 km thick in the segment of the Timor Trough studied by Karig et al. (1987). The unit records the deposition and building out of the continental slope and continental shelf of Australia from the Early Cretaceous to late Tertiary time.

The fourth stratigraphic sequence of the outer slope of the trough was deposited in progressively deeper water. The sediments grade upward from shelf carbonates to hemipelagic carbonate oozes representing the deflection of the Australian margin into the Timor Trough after the onset of subduction. The sequence averages 250 m, but varies in thickness and continuity between seismic lines (Figure 5).

The outer slope of the Timor Trough is cut by numerous normal faults. The faults decrease in displacement upward, indicating reactivation of ancestral faults as the slope began the flexure and descent into the trough. Montecchi (1976) interpreted the outer slope to also have reverse faults as seen in seismic lines in Figures 6 and 7. The lines described by Montecchi (1976) are 300 to 400 m east of the study area of Karig et al. (1987).

Trough Floor. The floor of the Timor Trough is filled by a wedge of horizontally stratified mass-wasting deposits (Figures 6, 7, and 8). In contrast to other trench and trough settings, the detailed bathymetry and closely spaced seismic lines of Karig et al. (1987) showed that the trough floor varies in depth and width over very short distances. A series of parallel seismic lines collected by Karig et al. (1987) with an approximate separation of 5 km shows that the trough floor sedimentary sequence can vary in width from 17 km on line K-L to less than 1 km on line D-C (Figure 9). The lack of continuity of the trench floor is a result of the shortening which is concentrated at the northern limit of the trench floor. Most of the shortening associated with plate convergence occurs at the principal thrust fault at the foot of the inner slope of the trough (Figures 6, 7, and 8). However, the closely-spaced parallel sections in Figure 9 show that compressive folding and thrusting occurs beneath the present trough floor and even on the lowermost portions of the outer slope. The seismic lines were correlated by Karig et al. (1987) to produce a structural map (Figure 10). The map shows that the folds are laterally continuous and are related to thrust faulting. The individual thrust sheets are 7 to 10 wide and extend along the trench for to 25 km. The faults typically dip to the north at 15° to 20°.

Inner Slope. In the small area of the Timor Trough studied by Karig et al. (1987), the inner (north) slope to the trough is composed two distinct parts, designated the upper-slope and lower-slope sections. The upper slope was generally marked by very low local relief on the bottom, with the seafloor gradient gently increasing from the continental shelf of Timor to the about 1,500 m water depth. Except for a thin surface veneer of sediments, no reflectors could be resolved from within the upper-slope areas. The lower-slope section extends from a seafloor depth of about 1,500 m to the trough floor, and consists of large folds and thrust sheets. The folds serve to dam downslope sediment transport and form small slope basins. The location of one such slope basin is shown in Figure 10.

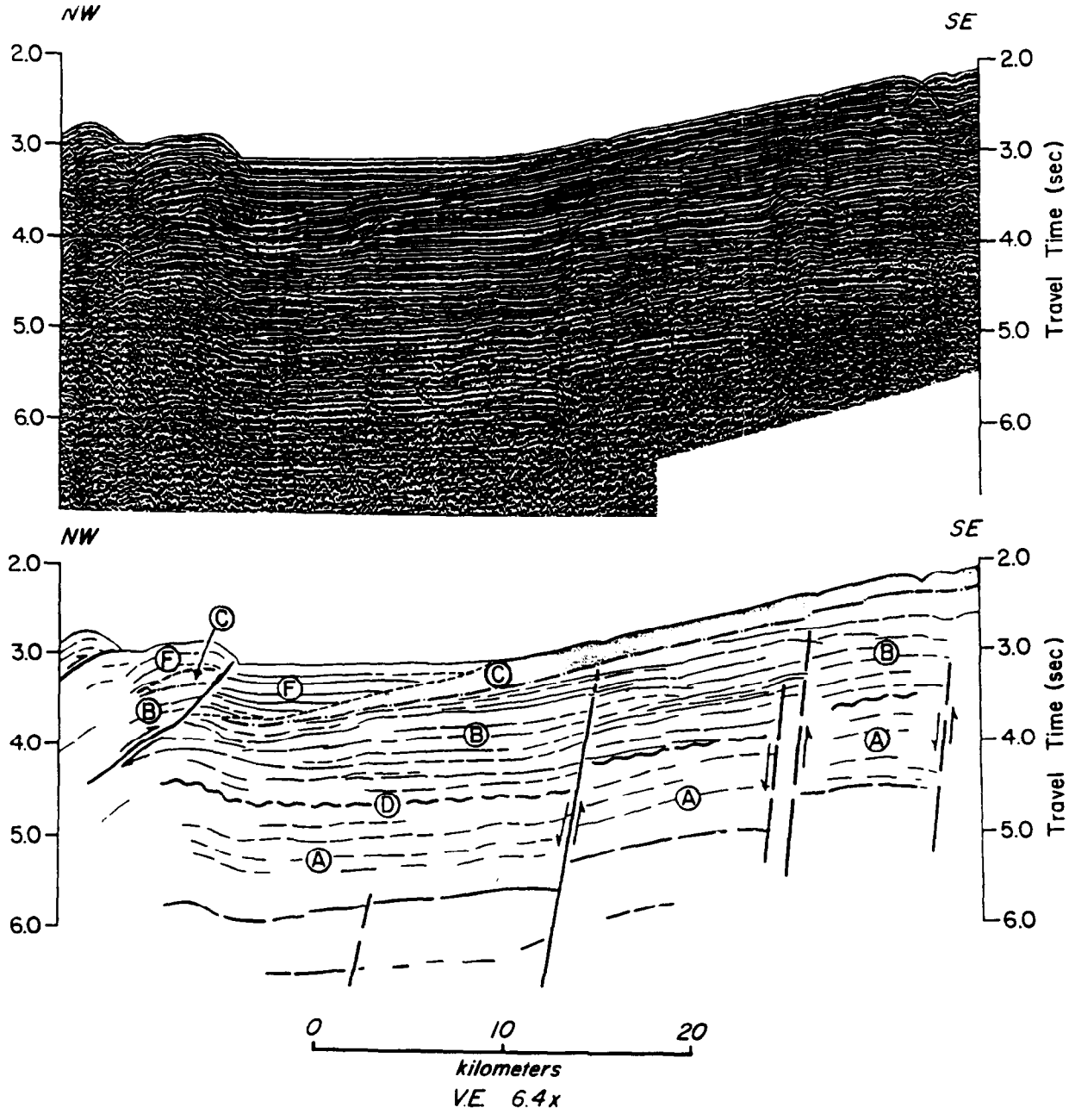

Figure 6. SEISMIC LINE AU-38F, TIMOR TROUGH

Seismic stratigraphy units: (A) Pre-rift strata, (B) Passive margin strata, (C) Outer slope strata, (D) Breakup unconformity, (F) Trough fill.

From Karig et al., 1987

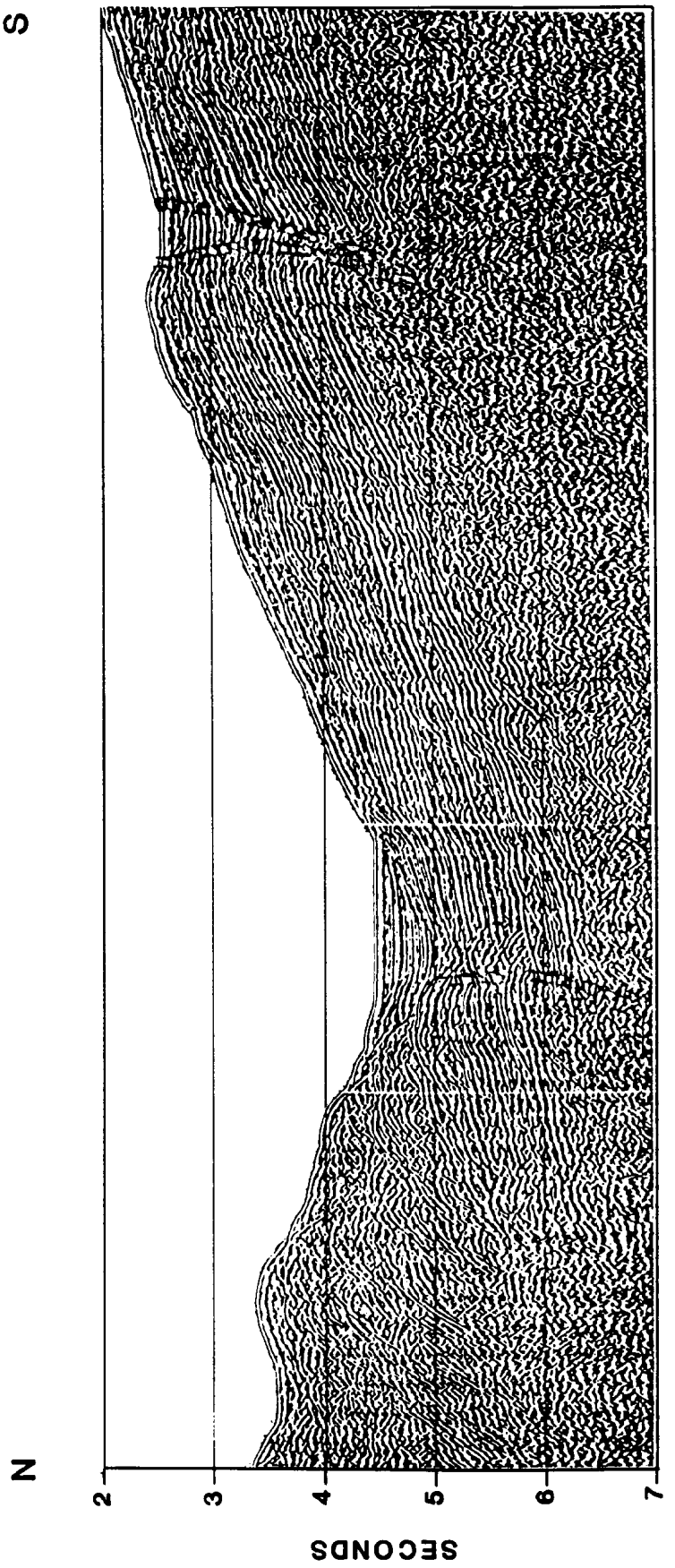

Figure 7. SEISMIC LINE IBA-25, TIMOR TROUGH

Approximate Location: 128°40'E

After Montecchi, 1976

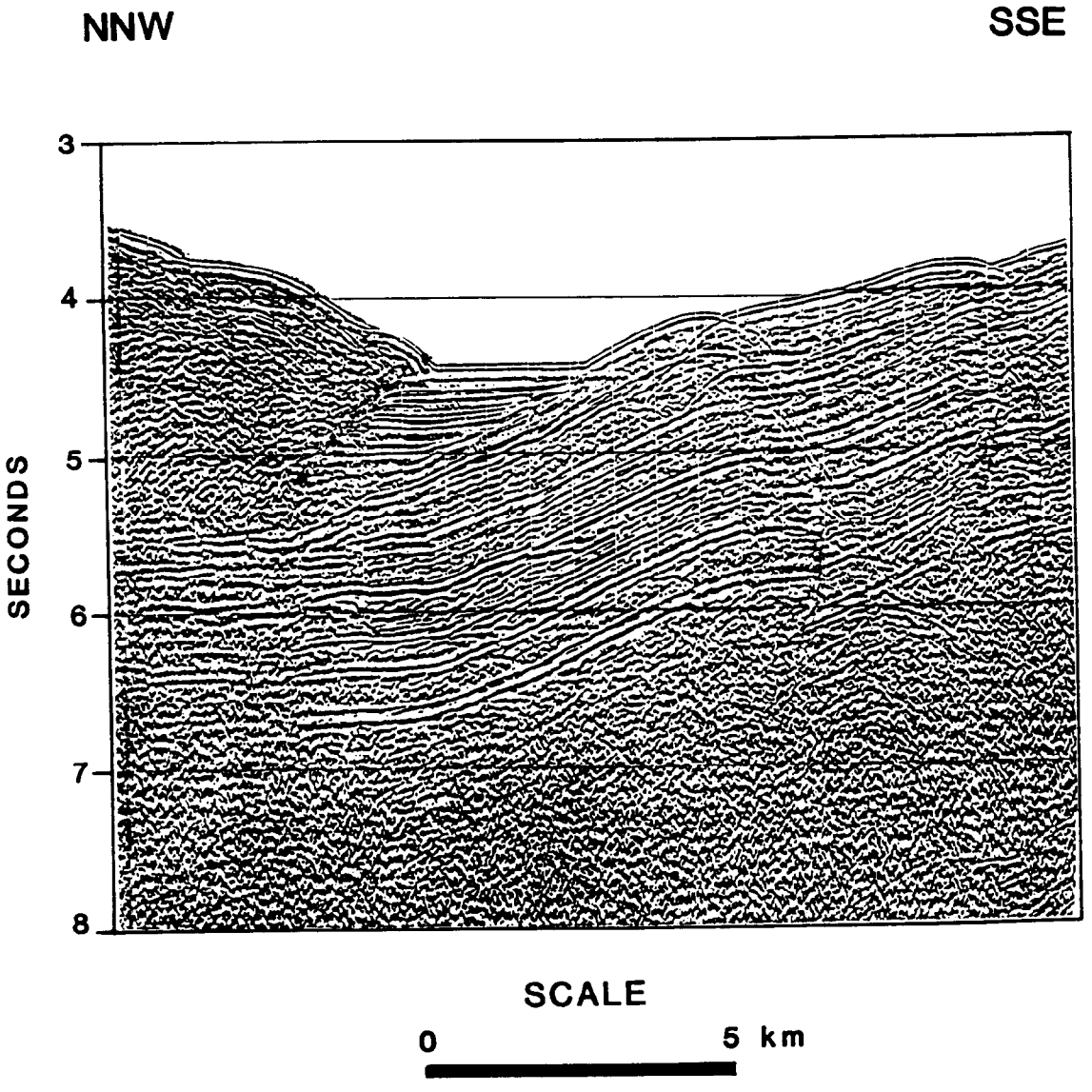

Figure 8. SEISMIC LINE TIS-2, TIMOR TROUGH
Approximate Location: 127°20'
After Montecchi, 1976

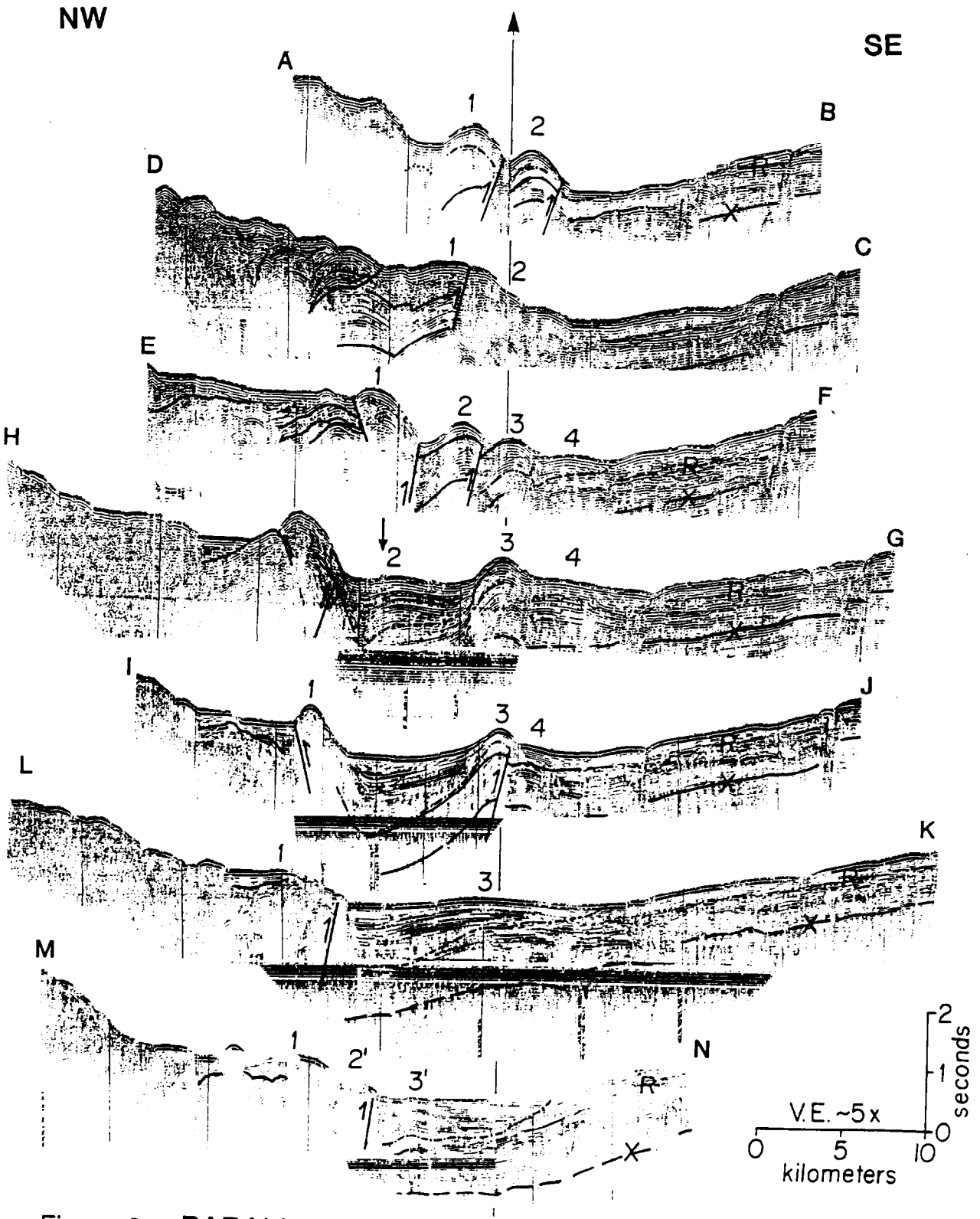

Figure 9. PARALLEL SEISMIC LINES, TIMOR TROUGH

Location shown in Figure 10. Numbers identify correlated anticlines. Vertical arrow is oriented N60°E

From Karig et al., 1987

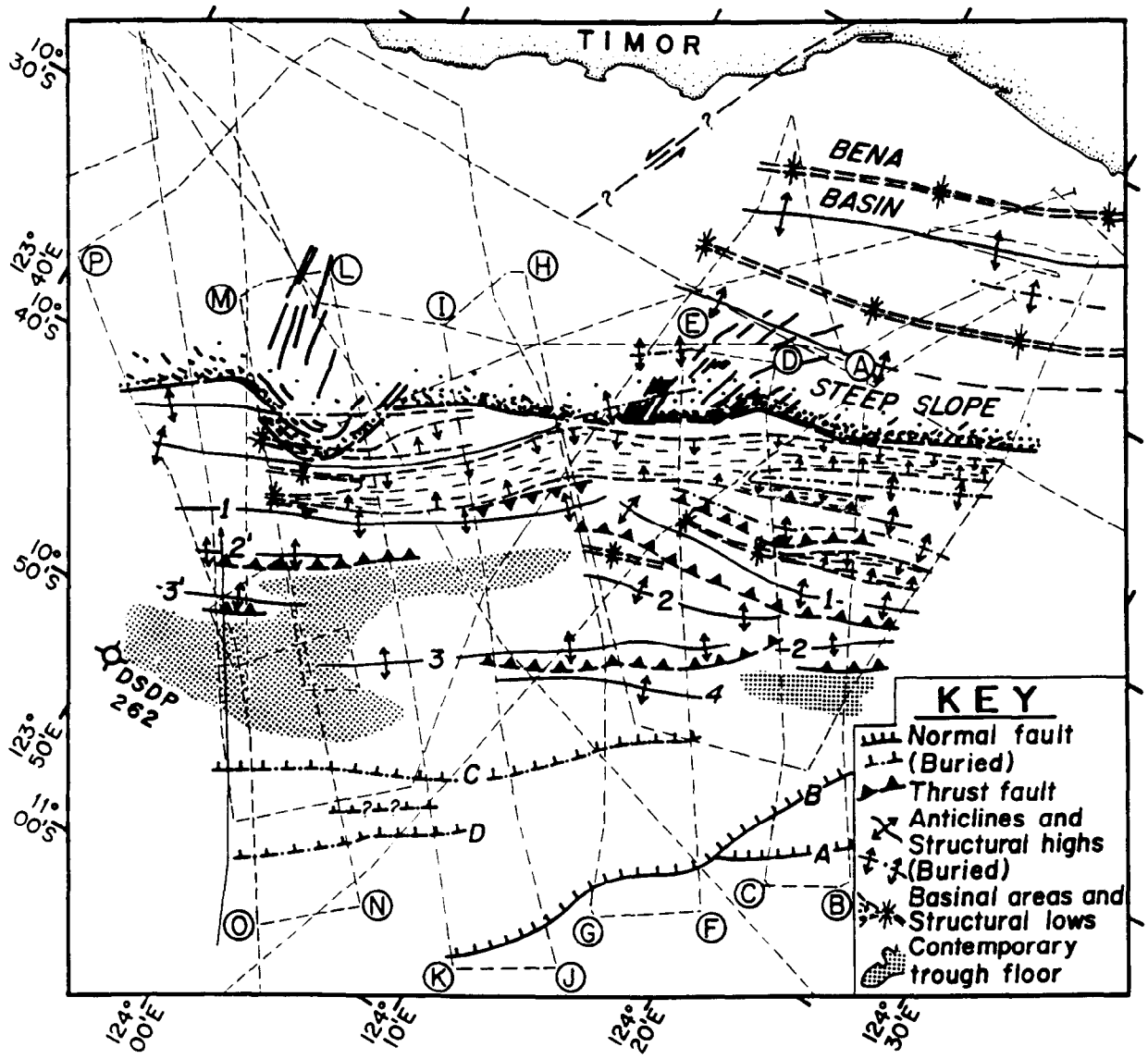

Figure 10. STRUCTURAL MAP OF THE SOUTHEASTERN PORTION OF THE TIMOR TROUGH

From Karig et al., 1987

The lack of coherent internal reflectors that was noted on the upper slope area appears to extend to the lower slope in available seismic lines from outside the area studied by Karig et al. (1987) (e.g., Figures 6 and 7). However, it is uncertain whether the lack of internal reflection in the adjacent, less studied areas is due to different sediment character, or to different seismic acquisition and processing parameters.

The two distinct slope types were interpreted by Karig et al. (1987) to reflect contrasts in the material being accreted. They postulated that the lack of coherent internal reflections in sediments of the upper slope indicated that the sediments were clay-rich, and were subjected to very small-scale deformation. The small-scale deformation disrupted sediment layering and homogenized the sediments, obliterating useful seismic reflecting horizons. The sediments composing the upper slope regimen were proposed to be trough fill and surficial hemipelagic sediments originally deposited on the continental rise of Australia. In contrast, the large thrust sheets of the lower slope which retain seismic coherence at depth were interpreted to consist of more competent material. Karig et al. (1987) suggested that the thrust sheets are composed of thick sections of continental slope and shelf deposits which had been scraped from the subducting plate. The accreted material of the lower slope was more thoroughly indurated, and thus failed along large thrust systems, rather than by internal shear and small-scale deformation as proposed for the upper slope.

The transition from the lower slope composed of ridges and thrust sheets in the area studied by Karig et al. (1987) to a smoother lower slope to the northeast was interpreted to indicate that subduction has not proceeded to as great a degree in the northeastern sections of the Timor Trough. By that interpretation, the northeastern sections of the trough are still subducting and accreting very fine-grained hemipelagic material.

Timor

The complex geology of Timor has resulted from the uplift of Tertiary marine sediments accreted onto an older sedimentary and metamorphic terrane. The accretion and uplift is due to subduction occurring in the Timor Trough. The island of Timor can be divided into two geological provinces approximately occupying the north and south halves of the island. The northern portion of the island is composed of a contorted array of lithologies of uncertain origin. Rocks exposed in the southern portion of Timor document the formation and development of the present subduction system.

The northern province of Timor consists of rocks from Permian to Tertiary age. The rocks include high-pressure metamorphics, pillow basalts, continental intrusives, and limestones (Hamilton, 1979). Karig et al. (1987) asserted that the rocks were of Asian affinities, and accumulated during very early stages of activity on the Banda Arc or its predecessor. However, Hamilton (1979) and Milson and Audley-Charles (1986) cited evidence that the rocks, particularly a pink Permian Limestone, can be related to similar rocks on Australia. Charlton (1989) noted that rocks of the northern geologic province are demonstrably allocthonous, being composed of obviously exotic rock types. Charlton proposed that the rocks

within the northern province which can be shown to be of Australian origin were originally part of the southern province. Displacement along left-lateral wrench faults during more recent times interposed fault slivers of rocks from the southern province into the northern province.

The basal unit of the southern geological province of Timor is the Kolbano Complex. Charlton (1989) reported that the base of the Kolbano Complex within the southern province decreases in age from the north to the south. The Permian Maubisse Formation, composed of fusilinid limestone is overlain by the Triassic Aitutu Babulu Formation composed of radiolarian calcilutite, and turbidites. To the south the Aitutu Babulu Formation grades into and interfingers with the red beds, marine silts and glauconitic sandstones of the Oe Baat Formation. Cretaceous radiolarian red clays of the Nakfunu Formation and Cretaceous to Paleogene calcilutite of the Boralalo Formation overly the regional Jurassic-Cretaceous breakup unconformity described by Karig et al. (1987). The Paleogene Ofu Formation is composed of thick deposits of foraminiferal cacilutites and calcareous mudstones and turbidites. The Miocene to Pliocene Batuputih Formation consists of similar calcilutites and conglomerates. This assemblage of rocks is tightly folded with abundant thrust faults of varying displacement. Karig et al. (1987) and Charlton (1989) interpreted the rocks of the Kolbano Complex to be continental rise, slope, and outer shelf sediments deposited on the Australian margin and subsequently shortened and folded by compressive forces resulting from the later collision processes.

The late Pliocene units overlying the Kolbano Complex record the collision and subduction of the Australian continental margin beneath the Eurasia Plate at the Timor Trough. The Bobonaro Scaly clay is a melange of exotic blocks principally from the Permian and Triassic units of the northern geological province in a highly sheared montmorilonite matrix. Deep-sea manganese nodules and pelagic red clays are also reported from the unit (Johnston and Bowin, 1981). The melange has been interpreted as resulting from rapid southward tilting of Timor in response to formation of the incipient subduction zone. However, the source of the volcanic ash which formed the clay matrix is problematic.

Continued subsidence in the early Pliocene resulted in deposition of the Batu Putih Limestone over the Bobonaro Scaly Clay (Figure 11). The Batu Putih Limestone is composed of deep-water calcilutite and constitutes the basal unit of the Viqueque Group. An intraformational unconformity dated by Milsom and Audley-Charles (1986) as approximately 3 Ma indicates the beginning of uplift of the unit. The Batu Putih Limestone deposition continued until the Pleistocene. Viqueque Turbidites and the Noel Marls were deposited in local depressions in the upper part of the Batu Putih Limestone. The exotics incorporated in the Viqueque Group decrease in age and transport distance upward in the unit. Clasts incorporated in the upper turbidites are from older Kolbano Complex rocks (Johnston and Bowin, 1981).

During the Pleistocene, shallow water deposits including coral reefs were emplaced above the Viqueque Group. Continued uplift into the present has exposed these Pleistocene reefs at elevations of 700 to 1,300 m (Karig et al., 1987). Terraces along the rivers of Timor also indicate continued uplift. The reefs and terraces suggest present uplift in excess of 1 m/my (Figure 11).

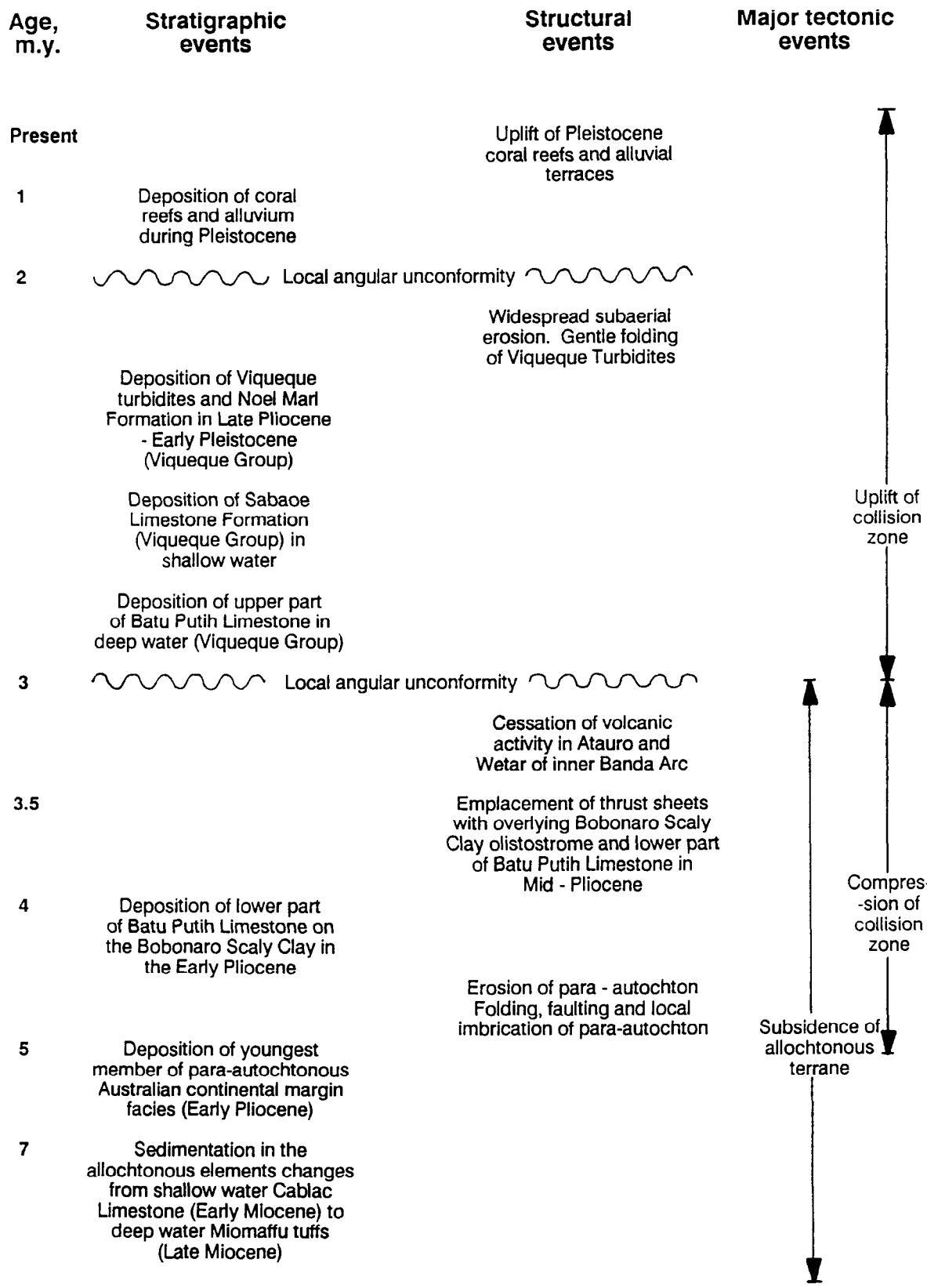

Figure 11. **NEOGENE GEOLOGIC HISTORY OF TIMOR**

Modified from Park, 1987

Timing and extent of deformation.

Karig et al. (1987) combined their seismic and seafloor morphology data with earlier work to arrive at qualitative estimates of convergence and uplift along the Timor Trough. Since most of the relative motion of the two plates is concentrated at the floor of the trench, uplift is most rapid there. Karig et al. (1987) estimated that each of the individual thrust slabs that they mapped rise 200 to 300 m in less than 10,000 yr by ramping along imbricate thrust faults. Slower uplift of 2 to 5 m/1000 yr is projected for the lower part of the accretionary prism. They postulated that the uplift rates determined from rates of thrusting may be augmented by sedimentary underplating from the subducted trough fill and continental margin sediments.

The Timor Trough differs from other modern collision zones in a number of features. The trough is comparatively deep, principally because of the small area of the exposed source terrane on Timor, and the lack of significant alluvial input from the Northwest margin of Australia. As a result of the relatively thin trough fill, large thrust sheets composed of indurated continental margin sediment are accreted, at least in the southwestern portions of the trough.

Sediments.

The floor of the Timor Trough was cored during Leg 27 of the Deep Sea Drilling Project (Veevers et al., 1974). Site 262 was located at 10°52.19'S, 123°50.78'E, near the southwest end of the trench (Figure 1). The site was selected to provide evidence on the age of formation of the Timor Trough. Additionally, it was hoped to identify the rocks causing a regionally extensive reflector on seismic profiles.

The hole at Site 262 was continuously cored to a depth of 442 m. Predominantly calcareous sediments of Pliocene to Holocene age were recovered (Figure 12). Upper units contain deep-water fossils indicating deposition at a water depth near that at present (2,298 m). Lower units were deposited in shallow water, continental shelf environments.

Unit 1

The uppermost sedimentary unit drilled at Site 262 was a 261.5 m thick section of grayish-olive and pale-olive, radiolarian and clay-rich nanofossiliferous ooze. Minor amounts of foraminfera-rich ooze and sand-sized detrital foraminiferal debris were identified. The radiolarian ooze was determined by bulk X-ray analysis to contain 42% calcite, 20% quartz, 10% montmorillonite, 10% mica, 8% aragonite, 4% magnesian calcite, 3% plagioclase, and 1% chlorite. The clay rich ooze made up about 30% of the section and was the dominant lithology between 147 and 195 m. The clay rich unit was compositionally similar as determined by bulk X-ray analysis (Cook et al., 1974).

The minor constituent of foraminifera-rich ooze was similar in make up to the radiolarian ooze, with forams taking the place of the radiolarians. Greenish-

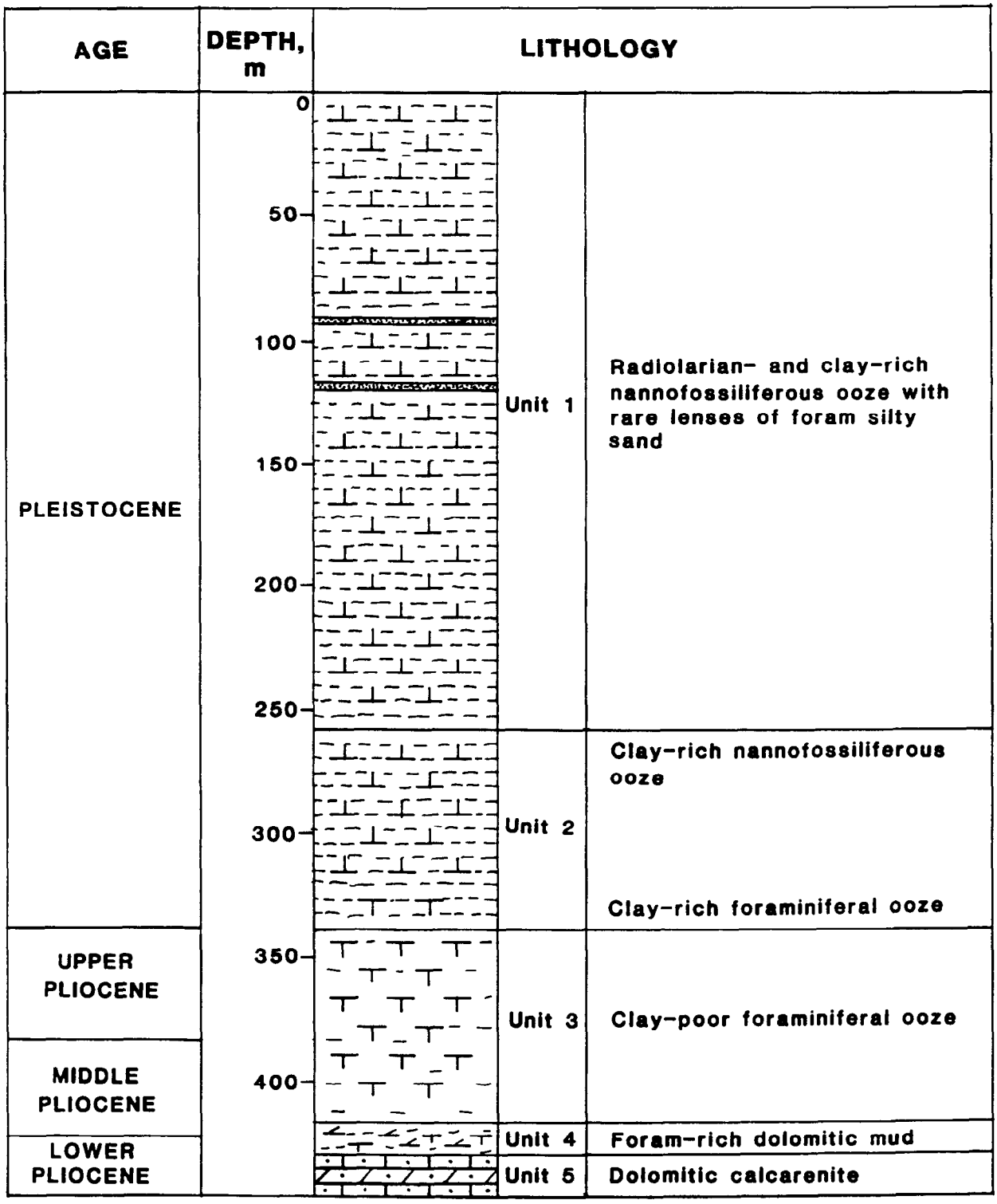

Figure 12. LITHOSTRATIGRAPHIC SUMMARY OF DSDP SITE 262, TIMOR TROUGH

After Veevers et al., 1974

gray detrital foraminferal sands occurred near the base of cores 10, 11, 12, and 16. The sands were composed of 85% foraminifera and 10% carbonate fragments.

Total carbon of the unit averaged 5%, with total organic carbon (TOC) averaging about 1%. The unit was composed of an average of 34% $CaCO_3$.

Unit 2

The next lower sedimentary unit at Site 262 consists of clay-rich nannofossil-rich ooze. Unit 2 extends from subbottom depths of 261.5 to about 337.5 m; the upper and lower contacts are gradational.

The Pleistocene unit is composed of about 60% nannofossils, 20% clay, 10% microcrystalline carbonates, and 5% foraminifera. The abundance of nannofossils decreases toward the bottom of the unit, while the proportion of foraminifera increases. Bulk X-ray analysis of the unit revealed a composition of: 55% calcite, 2% calcium dolomite, 16% aragonite, 10% quartz, 1% plagioclase, 2% kaolinite, 7% mica, 1% chlorite, and 5%montmorillonite. The total organic carbon content (TOC) of the unit averages 0.8%. Three grayish-white volcanic ash layers were recognized in the unit. The ash layers were composed of clay, and vitric and lithic fragments. One 1.5-cm pumice fragment was recovered.

Unit 3

A Pliocene unit composed of foraminiferal ooze was identified between 337.5 and 414 m at Site 262. The thickly bedded sediments of Unit 3 were more cohesive than overlying material, ranging up to semi-lithified. The average gross composition of the nannofossil-rich foraminiferal ooze of Unit 3 was determined from microscopic observation to be: 47% forams, 22% carbonate fragments, 19% nannofossils, 8% clay, and 2% quartz. Additionally, dolomite rhombs, pyrite, sponge spicules, plant debris, heavy minerals, and glauconite were reported. Bulk X-ray analysis revealed 61% calcite,. 13% calcian dolomite, 16% argonite, 7% quartz, 2% mica and traces of potassium feldspar, plagioclase, and kaolinite. Total organic carbon averaged 0.4% of the unit, and $CaCO_3$ constituted 72.4%.

Carbonate fragments increase from about 10% near the contact with Unit 2 to 30% at the base. Clay, foraminifers, and nannofossils decrease proportionally down-hole. The lower contact is sharp.

Unit 4

A thick-bedded gray to olive foraminifer-rich dolomitic mud was recovered between 414 and 427 m. Dolomite rhombs constitute 83% of the unit with 14% foraminifers and 2% clay. Pyrite, quartz and glauconite were also identified in the unit. The unit is quite lean in total organic carbon with only 0.2% average. The lower contact of Unit 4 was not recovered, but was inferred from a change in drilling rate.

Unit 5

A well lithified dolomitic shell calcarenite was recovered between about 427 and 442 m subbottom. Very low recovery was recorded for cores 46 and 47; the calcarenite was retained only in the core catcher.

The massively bedded calcarenite consisted of shallow marine foraminifera, molluscs, echinoderms, and sponge spicules in a matrix of sparry calcite and dolomite. Minor amounts of heavy minerals, clay and quartz were also identified.

Lithologic interpretation

Veevers et al. (1974) interpreted the sedimentary sequence at Site 262 to represent a very rapid deepening from water depths of less than 30 m to over 2,000 m in the Pliocene.

The basal calcarenite was deposited in shallow water. The shallow-water origin is indicated by the foraminifera population and the mollusc and echinoderm remains which were broken and rounded by wave action. The moderate sorting of the skeletal debris and low clay content also indicate a high-energy depositional environment.

The foraminifera which constitute 14% of the dolomitic mud of Unit 4 were exclusively very shallow-water benthonic forms. It is not clear whether the dolomite rhombs which make up 83% of the unit were recrystallized from primary dolomite were formed from alteration of micrite.

The nannofossil-rich foraminiferal ooze in Unit 3 records the rapid Pliocene foundering. Near the base of the unit, benthonic foraminifera indicating water depths of less than 30 m dominate. The benthonic foraminifera disappear in core 42 (390 m) and are replaced with deep-water varieties. Veevers et al. (1974) interpreted that water depth during deposition of the sediments in the top of Unit 3 were similar to that at present.

The nannofossil ooze which make up Units 1 and 2 were formed above the regional carbonate compensation depth in an environment which was similar to that in the present Timor Trough. Identifiable remains from these units are dominated by pelagic radiolarians, foraminifera and diatoms. Clay makes up 10 to 25% of these units. The source of the clay was the island of Timor which was emergent during the Pleistocene. The very high sedimentation rate in the Quaternary of 150 m/my probably reflects both direct sedimentation and slumping of shallower pelagic material from the trough walls to the axis. The surficial foraminifera sands of Unit 1 have very little clay and do not display graded bedding. These sands are interpreted to have resulted from current winnowing removing the fines from the material.

Density and Porosity

A suite of physical property measurements including bulk density, acoustic velocity, porosity and shear strength were taken on the cores recovered from Site 262. Bulk density data tabulated by Rocker (1974) are presented as the plot marked by stars in Figure 13. Density of the sediments increased irregularly from 1.50 g/cm^3 at the seafloor to 2.10 g/cm^3 at the bottom of the hole. Veevers et al.

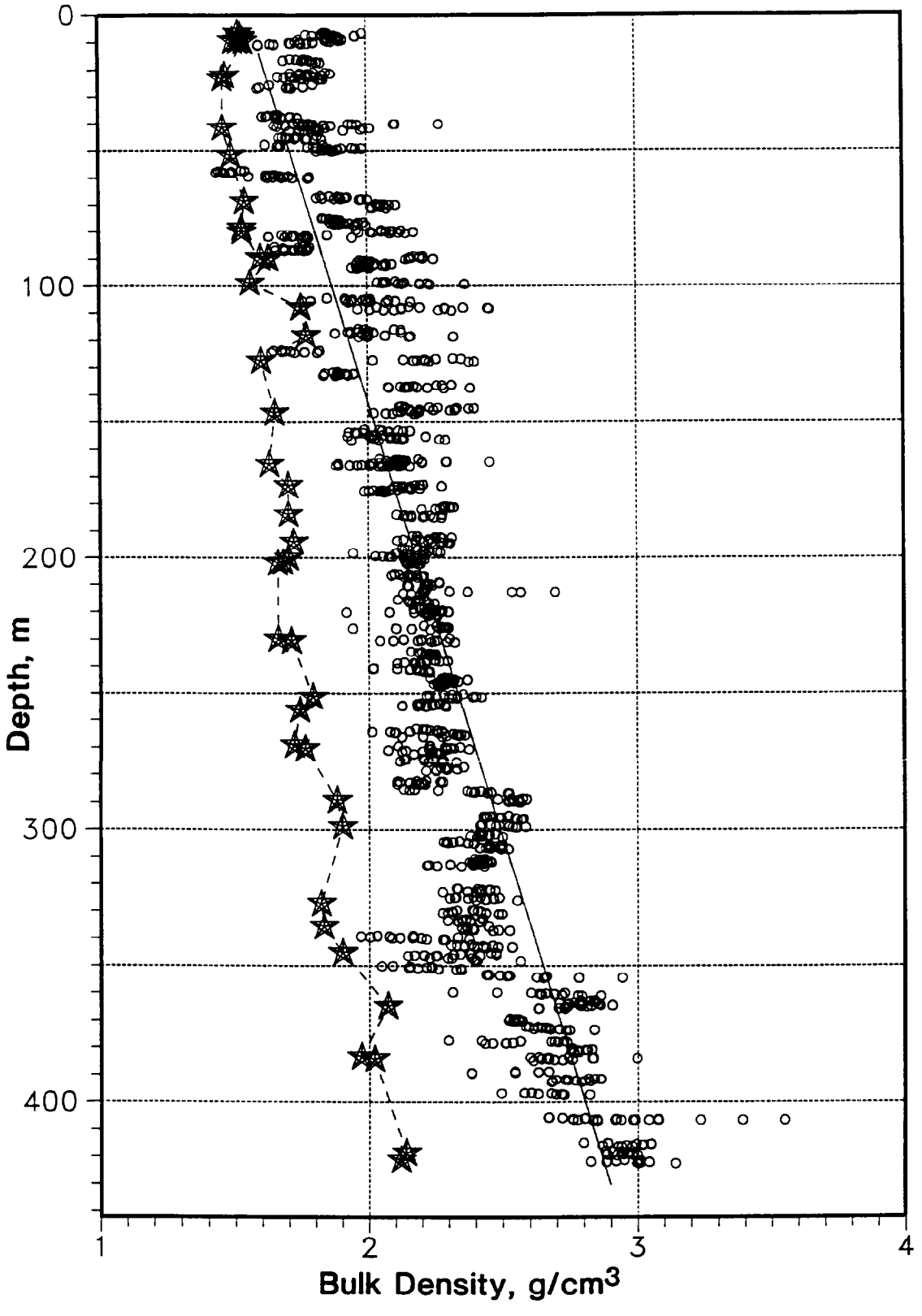

Figure 13. **BULK DENSITY OF DSDP SITE 262 SEDIMENTS**

Data from: Rocker, 1974 (★), and Veevers et al., 1974 (○)

(1974) indicated that the wide scatter of bulk density measurements in the upper 250 m of the recovered cores may have been caused by gas expansion disturbance. However, they noted that the density of very distorted sediment in portions of cores with a high level of gas expansion were similar to areas of the cores which were undisturbed by gas expansion. Occasionally, the density of badly disturbed areas of the cores was significantly higher than measurements from undisturbed sections. The perplexing situation was assessed as follows: "If the volume of dissolved gas in these adjacent areas (of similar sediment) varied, this would indicate that the sediment containing more dissolved gas exists in situ at higher density, or the identified density variations would the result of disturbance which causes consolidation of the more gaseous sediments, a process which is difficult to explain."

Veevers et al. (1974) presented plots of measured GRAPE (gamma-ray attenuation porosity estimator) bulk density for each of 47 cores recovered at Site 262 . We digitized the bulk density graphs published by Veevers et al. (1974) and present the data from all cores compiled into one graph for Site 262 (Figure 13). The data reported for each core are represented in Figure 13 by the circles and accompanying regression line. In Figure 13 the reported bulk-density values increase from 1.55 g/cm^3 at the seafloor to about 2.8 g/cm^3 at 420 m subbottom. These values are in disagreement with the range quoted in the text of Veevers et al. (1974) and tabulated by Rocker (1974) of 1.5 to 2.1 g/cm^3.

A corresponding discrepancy exists between the porosity values for Site 262 which were cited in the text of Veevers et al. (1974) and those obtained from the accompanying bulk density graphs (Figure 13). Porosity, bulk density, and grain density are related by the equation:

$$\textit{bulk density} = \textit{porosity} + \textit{grain density}(1 - \textit{porosity}).$$

Veevers et al. (1974) stated that porosity decreased regularly from 68% at the seafloor to 38% at 420 m. Using the bulk density range of 1.5 g/cm^3 to 2.1 g/cm^3 for the hole, the grain density corresponding to the cited porosity values is 2.5 g/cm^3 to 2.6 g/cm^3. Such grain density values are reasonable for sediments composed of calcite, dolomite, and silica. In contrast, if the porosity range cited in the text by Veevers et al. (1974) (38% to 68%) is applied to the bulk density data presented in the graphs in the site summary sections of Veevers et al. (1974), grain density values range from 2.7 g/cm^3 at the seafloor to 4.1 g/cm^3 at 420 m. While some amount of pyrite and other heavy minerals was noted in core description, the amount reported was insufficient to increase grain density of the sediment to 4.1 g/cm^3. Over 60% of a calcareous sediment would have to be composed of pyrite with a density of 5 g/cm^3 to obtain a sediment grain density of 4.1 g/cm^3. Since such a high grain density is unlikely for the Site 262 sediments, the bulk density data reported in the core summaries in Veevers et al. (1974) (circles in Figure 13) are probably not as accurate as those reported by Rocker (1974) (stars in Figure 13).

Seismic Velocity

Gas expansion of cores 2 - 33 precluded seismic velocity measurements of those cores. It was reported that the acoustic signal could not picked up by the receiving transducer in the cores noted for gas presence. The DSDP scientists reported that the sonic velocity apparatus failed even in portions of the cores which were relatively undisturbed by gas expansion.

Seismic velocity of the surficial sediments (core 1) was measured to be 1.5 km/s. Below the gassy interval, sonic velocity increased from 1.65 km/s at 315 m to about 1.8 km/s in the soft sediments. The sonic velocity measured from the semi-lithified sediments was somewhat higher, ranging up to 2.4 km/s at 413 m.

Two prominent seismic reflectors were noted in regional seismic lines from the Timor trough. The more shallow reflector was present at 0.45 sec subbottom at Site 262. Based on drilling results and physical property analysis of the recovered cores, the prominent reflector was identified as corresponding to the well lithified shell calcarenite penetrated at 427 m (cores 46 and 47).

Heat flow

Down-hole temperature measurements at Site 262 indicate a low heat flow regime. Bottom water temperature was measured on duplicate runs to be 2.67°C (Erickson, 1974). A temperature of 10.46°C was recorded at a subbottom depth of 233.5 m. These data yield a geothermal gradient of 3.44°C/100 m for Site 262. A mean thermal conductivity value of 0.00256 cal/cm sec °C was obtained from 11 sediments samples from 229 to 290 m depth. The product of the geothermal gradient and the mean thermal conductivity is the heat flow, which is 0.88 cal/cm^2 sec (0.88 HFU). Erickson (1974) noted that the heat flow value is relatively low. The very rapid sediment accumulation during the Pliocene and Pleistocene would have the effect of lowering heat flow. Erickson (1974) estimated that a crustal heat flow of about 1 HFU exists beneath Site 262, with the high sedimentation rate depressing the heat flow to the observed value. Erickson (1974) further speculated on the presence of a body of salt beneath Site 262. The presence of salt beneath Site 262 is suggested by the downhole increase in pore water salinity (Cook, 1974). Erickson (1974) noted that the high thermal conductivity of salt causes a salt body to focus heat flow. Thus, the heat flow of sediments overlying a salt body would be elevated. The low heat flow values registered at Site 262 suggested to Erickson (1974) that a discrete salt body does not directly underlie the drillhole. He proposed that the salt body may be offset laterally somewhat from the location of the drill hole, close enough to increase the salinity of the pore water, but restricting the heat-flow signature to sediments directly over the salt mass. Alternatively, Erickson (1974) indicated that the presumed salt mass beneath Site 262 may consist of a continuous layer rather that a discrete body. A laterally extensive salt layer of constant thickness would not elevate heat flow of the overlying sediments, and thus is consistent with the observed heat flow

Pore water geochemistry

The geochemistry of the pore water from cores drilled at DSDP Site 262 was determined by Cook (1974). The continuous coring and good recovery of cored sediments permitted very closely spaced sampling of sediment and pore water (Table 1).

The three most significant trends in pore water and sediment chemistry noted by Cook (1974) are displayed in Figure 14. Salinity of the pore water remains near that of sea water (36.5 ppt) to a depth of about 240 m, and then increases to 53 ppt at total depth. The alkalinity profile increases to a maximum of 93 meq/L at 50 m before diminishing rapidly to about 36 meq/L at 120 m. After a brief increase in alkalinity to 45 meq/L at 170 m depth the alkalinity quickly diminishes to 2 meq/L at 340 m. The carbonate fraction of the sediment increases in a manner parallel to the pore water salinity reaching a maximum expressed as 38% CO_2.

Salinity. The salinity increase is reflected in consistent increases of various cations and anions with depth. Chloride, calcium, strontium, and lithium increase downhole while magnesium and phosphate decrease with depth. Other inorganic pore-water constituents vary in concentrations in patterns that appear to be unrelated to sediment depth. Cook (1974) indicated that the most plausible explanation for the regular increase in salinity with depth is the presence of underlying salt. Citing similar examples of anomalous salinity with depth from the Mediterranean, Cook (1974) nonetheless noted that no other evidence for an evaporite layer at a greater subbottom depth existed. However, the shallow marine character of the sediments near the base of the hole is consistent with an evaporite-forming depositional setting.

Alkalinity. The rapid rise in alkalinity with depth and the progressive downhole decrease was reported by Cook (1974) to indicate microbial degradation of organic carbon. Such an alkalinity profile was reported by Claypool and Kaplan (1974) to be characteristic for bacterial fermentation of organic matter, a routine stage in the diagenesis of organic-rich marine sediments. As reported by Claypool and Kaplan (1974) and Berner (1980), the pore water alkalinity increase is due to the conversion of organic matter to CO_2. At the pH values typical of marine pore waters, CO_2 is present as bicarbonate (HCO_3^-) which is measured analytically as alkalinity.

Organic geochemistry

McKirdy and Cook (1980) documented the organic geochemistry of sediments cored from Site 262. In addition to total organic carbon testing, which had also been reported by Bode (1974), they performed analyses on the bitumen and kerogen components of the sediments. Extractable organic matter (EOM) was determined from the weight of the non-volatile portion of benzene and methanol extracts of the sediments. The extract was separated into aliphatic hydrocarbons, aromatic hydrocarbons, and polar compounds by column chromatography with an alumina adsorbent. Extracted sediments were treated with hydrochloric and

Table 1.

PORE WATER GEOCHEMICAL DATA, DSDP SITE 262
After Cook (1974)

Core	Depth m	Salinity ppt	Alkalinity meq/L	Sulfate ppm
Sea Water	0	34.6	2.49	2750
1	3.5	33.6	22.48	500
2	9.5	36.3	73.22	50
3	18.9	37.4	89.39	50
4	27	37.4	90.32	50
5	38	37.4	87.1	100
6	50.5	38	92.86	50
7	52.5	37.4	82.21	50
8	69.5	36.6	76.92	100
9	77.5	36.3	65.59	50
10	81	36.3	63.64	50
11	98	35.5	53.37	50
12	107.5	35.2	50.64	50
13	109.5	35.2	45.36	100
14	120.4	34.9	36.27	200
15	136	35.2	47.07	100
16	145.5	35.8	50.44	50
17	156.4	36.3	52.59	50
18	161.5	36.3	48.19	50
19	173.9	36	49.97	50
20	180.4	37.1	51.22	50
21	193	36.8	46.92	50
22	201	36.8	39.59	50
23	212	36.8	28.05	100
24	221.5	36.6	19.45	100
25	229.5	36.8	24.14	50
26	239	37.7	15.73	50
27	247	38.2	11.14	50
28	255	38.5	14.47	50
29	267.5	38.5	5.77	50
30	277	38.5	9.74	240
31	288	39.9	5.96	50
32	297.5	39.6	4.2	50
33	307	41.5	4.69	140
34	313.5	41.5	4.3	50
35	326	42.6	2.93	50
36	335.5	43.7	3.03	240
37	345	43.7	1.96	50
38	353	44.6	2.35	100
39	362.5	47.3	2.93	50
40	372	45.6	1.96	100
41	383	49.8	1.37	470
42	391	48.1	0.88	750
43	396	48.1	0.98	930
44	407	51.4	1.37	820
45	421	53.1	1.96	850

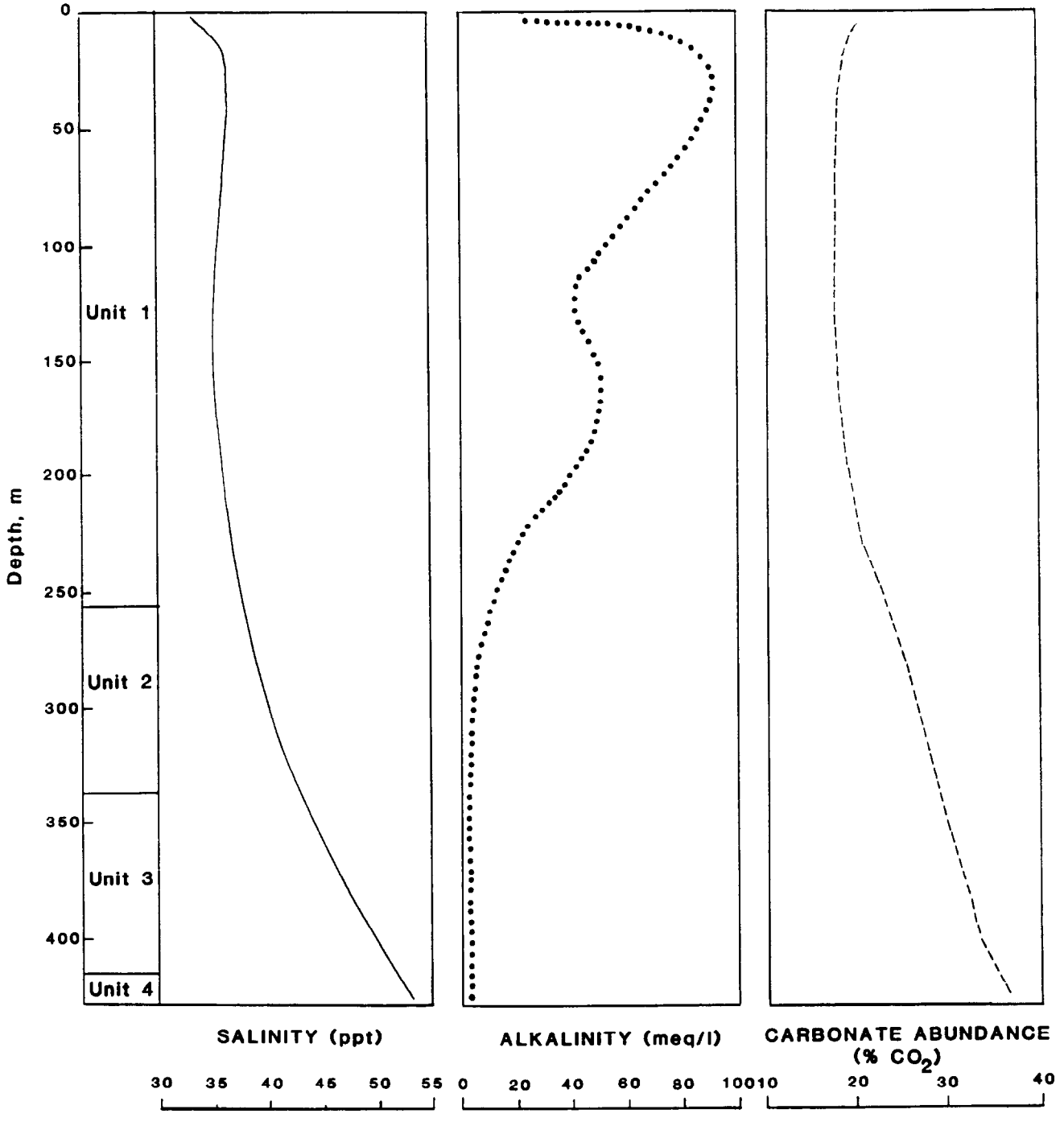

Figure 14. GENERALIZED GEOCHEMICAL TRENDS, DSDP SITE 262

hydrofluoric acid to dissolve the mineral matrix leaving kerogen for analysis. Kerogen was subjected to elemental analysis, and $\delta^{13}C$ determination.

Organic carbon content (TOC) of the Site 262 sediments decreases from about 0.6% at 3.5 m depth to 1.46 % at 52.2 m (Figure 15, Table 2). The TOC values for the sediments then decrease irregularly to 0.81% at 345 m at which point the values drop dramatically. From 352 m to the bottom of the hole, TOC values average 0.5%. McKirdy and Cook (1980) attributed the rapid increase in TOC values at 350 m to be a result of rapid subsidence noted by Veevers (1974). McKirdy and Cook (1980) projected that the rapidly increasing depth enhanced preservation by leading to increased sedimentation rates and restricted water circulation.

Carbon Isotopes. Isotopically heavy organic matter in the deeper sediments of Site 262 (Figure 15) were interpreted to indicate marine source for the carbon (McKirdy and Cook, 1980). Lighter isotopic signatures near the sea floor were interpreted as evidence of terrestrial input. McKirdy and Cook (1980) noted that some of the observed changes in $\delta^{13}C$ or the Site 262 organic matter may reflect changes in water temperature rather than source variation.

McKirdy and Cook (1980) interpreted the $\delta^{13}C$ values illustrated in Figure 15 to indicate two distinct clusters, with the $\delta^{13}C$ values between 80 and 170 m subbottom being significantly depleted (more negative) in ^{13}C. They indicated that the lower $\delta^{13}C$ values in that depth range indicated a depositional pulse of terrigenous material. The dashed line on Figure 15 is the 6th-degree polynomial line of best fit for the data. The best fit line with an equivalent r^2 value of 0.71 suggests agreement with McKirdy and Cook (1980) that $\delta^{13}C$ values of the organic matter is depleted in the middle of Unit 1 (0 - 261.5 m subbottom). Alternatively, the $\delta^{13}C$ pattern shown in Figure 15 could also represent a general increase in $\delta^{13}C$ values down hole with considerable scatter.

While changes in source characteristics could account for the general decrease in the heavier isotope uphole, other mechanisms could affect the isotopic signature similarly. In view of the reports of abundant methane in sediments above 300 m subbottom depth, the isotope change may reflect preferential extraction of the lighter isotope to form biogenic methane, leaving the remaining organic matter depleted in the lighter isotope resulting in a greater (less negative) net $\delta^{13}C$ value.

Extractable organic matter. The extractable organic matter content of the Site 262 sediments decreases regularly downhole (Figure 16). Since TOC values also decrease down hole, the decrease in EOM could conceivable be a relic feature of the TOC trend. However, as seen in the right-hand graph in Figure 16, EOM content is decreases down hole even when normalized to TOC.

McKirdy and Cook (1980) proposed that the TOC trends and EOM trends are related. They interpreted the high TOC values to indicate periods of greater primary productivity and/or better preservation. While their reasoning was not explicitly detailed in the paper, it could be argued that the increases in TOC attributed to greater preservation due to high sedimentation rates were due to the presence of more easily oxidized type II kerogen. That is, the more refractory

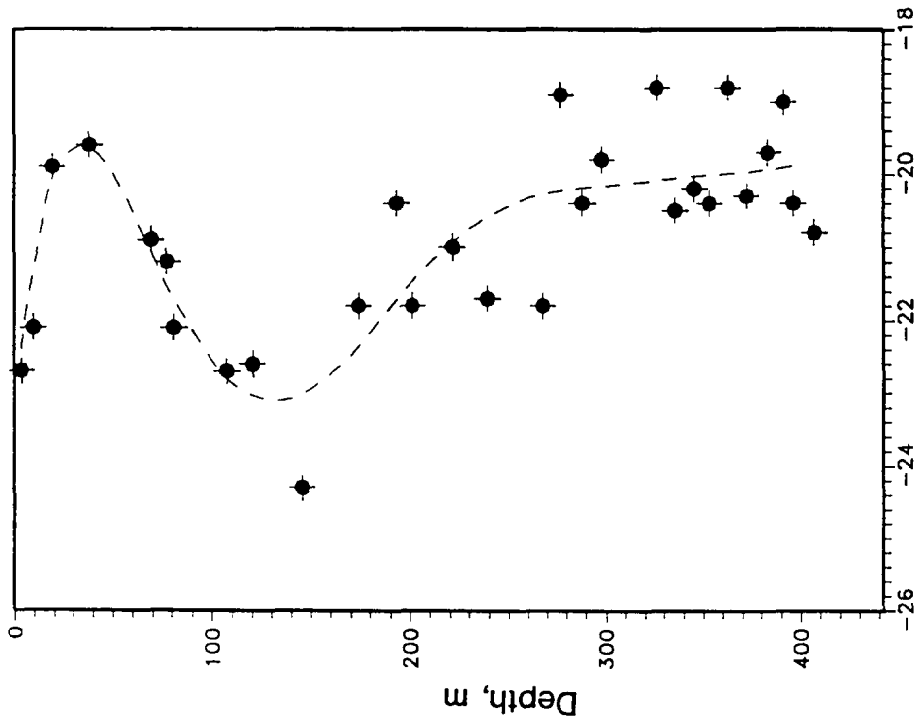

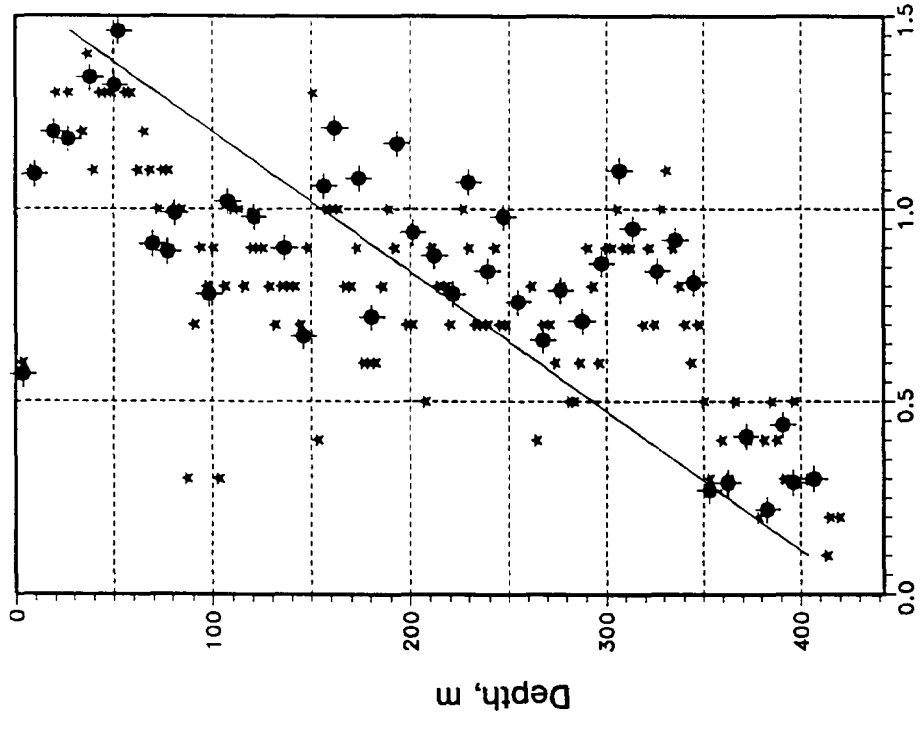

Figure 15. ORGANIC CARBON AND ISOTOPE CONTENT, DSDP SITE 262

Data from Bode, 1974 (*), and McKirdy and Cook, 1980 (+)

Table 2.

ORGANIC GEOCHEMICAL DATA, DSDP SITE 262

After McKirdy and Cook (1980)

Depth m	TOC %	$S^{13}C$ %	EOM ppm	EOM/TOC x 10^4	HC ppm	HC/TOC x 10^3	HC/EOM x 10^2	H/C	O/C
3.5	0.57	-22.7	-	-	-	-	-	-	-
9.5	1.09	-22.1	-	-	-	-	-	-	-
19	1.2	-19.9	1585	132.08	35	2.92	2.21	1.09	0.42
27	1.18	-	1425	120.76	37	3.14	2.6	-	-
38	1.34	-19.6	-	-	-	-	-	-	-
50.5	1.32	-	870	65.91	8	0.61	0.92	-	-
52.5	1.46	-	-	-	-	-	-	-	-
69.5	0.91	-20.9	1087	119.45	29	3.19	2.67	1.18	0.4
77.5	0.89	-21.2	1152	129.44	12	1.35	1.04	-	-
81	0.99	-22.1	-	-	-	-	-	-	-
98	0.78	-	-	-	-	-	-	-	-
107.5	1.02	-22.7	1042	102.16	57	5.59	5.47	1.21	0.32
120.4	0.98	-22.6	-	-	-	-	-	-	-
136	0.9	-	-	-	-	-	-	-	-
145.5	0.67	-24.3	367	54.78	-	-	-	-	-
156.4	1.06	-	1155	108.96	19	1.79	1.65	-	-
161.5	1.21	-	1362	112.56	25	2.07	1.84	1.16	0.34
173.9	1.08	-21.8	-	-	-	-	-	-	-
180.4	0.72	-	-	-	-	-	-	-	-
193	1.17	-20.4	-	-	-	-	-	-	-
201	0.94	-21.8	922	98.09	7	0.74	0.76	1.2	0.33
212	0.88	-	-	-	-	-	-	-	-
221.5	0.78	-21	751	96.28	6	0.77	0.8	-	-
229.5	1.07	-	-	-	-	-	-	-	-
239	0.84	-21.7	412	49.05	6	0.71	1.46	-	-
247	0.98	-	754	76.94	9	0.92	1.19	-	-
255	0.76	-	715	94.08	-	-	-	1.09	0.32
267.5	0.66	-21.8	-	-	-	-	-	-	-
277	0.79	-18.9	-	-	-	-	-	-	-
288	0.71	-20.4	364	51.27	12	1.69	3.3	-	-
297.5	0.86	-19.8	834	96.98	5	0.58	0.6	1.28	0.32
307	1.1	-	-	-	-	-	-	1.35	0.27
313.5	0.95	-	468	49.26	12	1.26	2.56	-	-
326	0.84	-18.8	772	91.9	38	4.52	4.92	1.26	-
335.5	0.92	-20.5	752	81.74	17	1.85	2.26	-	-
345	0.81	-20.2	596	73.58	14	1.73	2.35	-	-
353	0.27	-20.4	-	-	-	-	-	-	-
362.5	0.29	-18.8	152	52.41	8	2.76	5.26	1.36	0.28
372	0.41	-20.3	-	-	-	-	-	-	-
383	0.22	-19.7	152	69.09	8	3.64	5.26	-	-
391	0.44	-19	215	48.86	6	1.36	2.79	1.27	0.26
396	0.29	-20.4	123	42.41	5	1.72	4.07	-	-
407	0.3	-20.8	221	73.67	9	3	4.07	1.25	0.35

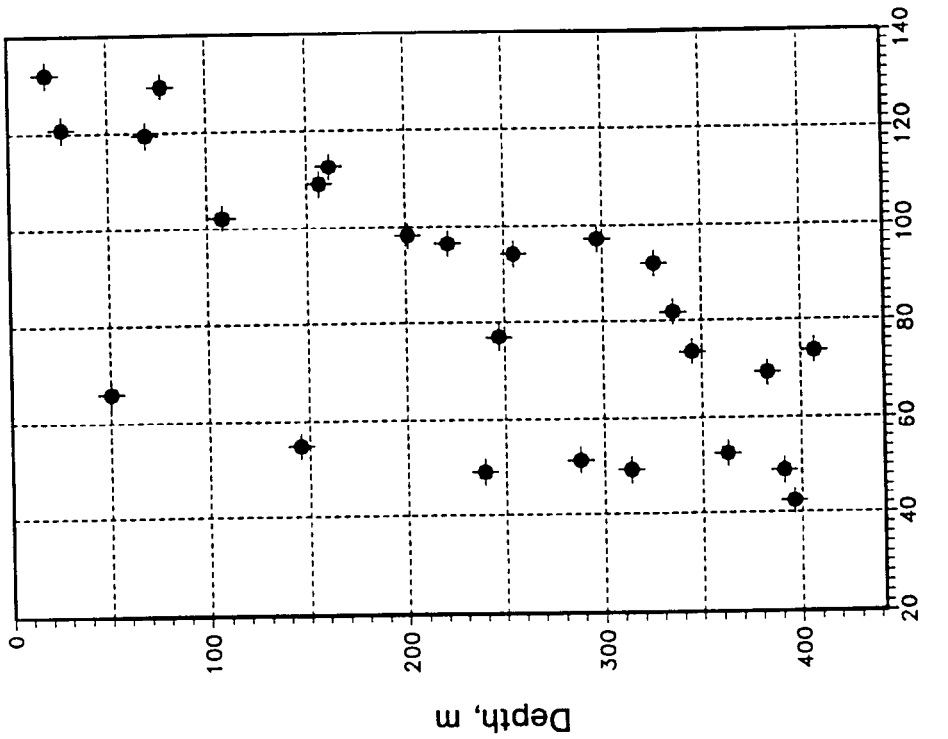

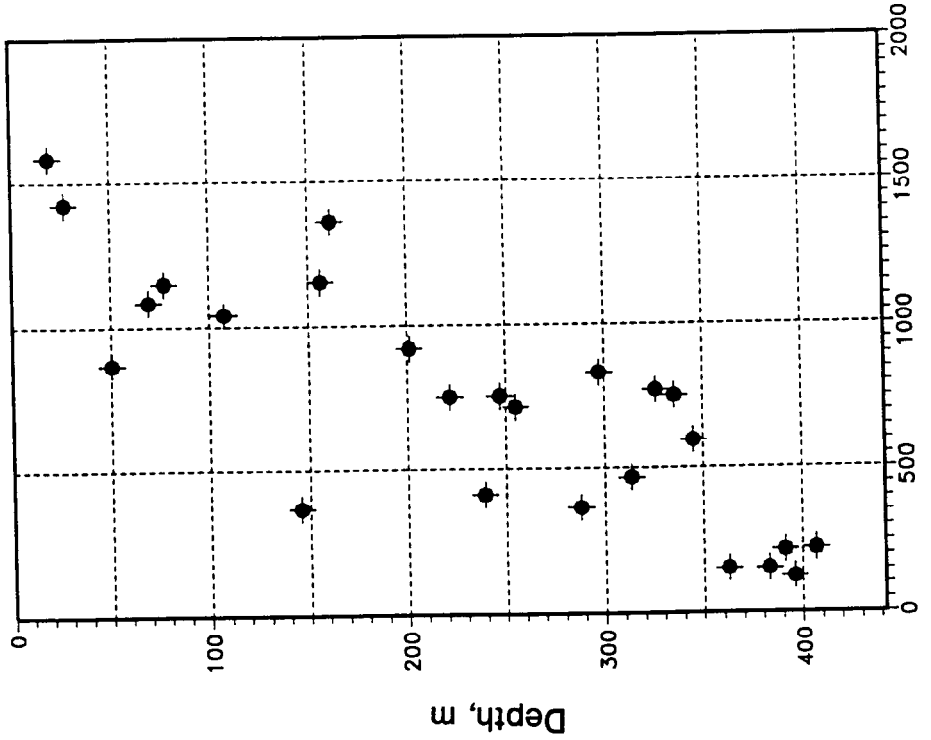

Figure 16. EXTRACTABLE ORGANIC MATTER, DSDP SITE 262

Data from McKirdy and Cook, 1980

type III kerogen would be substantially preserved throughout the sediment column, but only in conditions favorable for preservation could substantial change to TOC occur in the form of admixture of type II kerogen to the preserved material. Type II kerogen tends to give higher EOM yields than type III at a similar maturity level (Tissot and Welte, 1984). Thus, the probable relative abundance of type II kerogen in zones of high TOC could increase EOM to the extent that it would be obvious even when normalized to TOC as in Figure 16.

Thermal maturation of sediments increases the hydrocarbon extent of the sediments (Tissot and Welte, 1984). In Figure 17 the hydrocarbon content of the EOM is diagrammed. In the left-hand graph the absolute amount of hydrocarbons in sediment extracts is seen to decrease. However, when normalized to EOM values, the hydrocarbon content of the extracts appears to have little relationship to depth, or perhaps a slight increase with depth. However, only 0.5% to 4.5% of the extractable organic material is composed of hydrocarbons, indicating that these sediments are very much thermally immature.

McKirdy and Cook (1980) used a number of other indicators derived from the extract fraction of the Site 262 sediments to bolster their claim that a greater proportion of terrigenous organic matter was deposited and between 50 and 150 m depth within Unit 1.

Kerogen. The hydrogen content of kerogen increases down hole at Site 262 (Figure 18). A simultaneous decrease in oxygen content of the kerogen is seen in Figure 18. Since terrestrial type III kerogen is higher in oxygen and lower in hydrogen contents than marine type II kerogen (Tissot and Welte, 1984), the kerogen composition data agree with the bitumen composition data of McKirdy and Cook (1980) in suggesting a greater input of terrestrial organic material in the Pleistocene in Units 1 and 2.

We have plotted the kerogen composition data of McKirdy and Cook (1980) on a van Krevelen diagram in Figure 19. The fields in the diagram corresponding to types I, II, and III kerogen were derived from Tissot and Welte (1984). Figure 19 shows that the organic matter from Site 262 is a mixture of types II and III and of low maturity. In the right-hand portion of Figure 19 the kerogen composition of the Site 262 sediments is graphed, and each data point is identified by subbottom depth. The Kerogen composition data from Unit 1 form a cluster of points which is consistently more terrigenous than the grouping of values from Units 2 and 3 sediments.

Hydrocarbon Generation Potential

The sediments of the Timor Trough study region have significant organic carbon. Present burial depths of the sediments thus far cored and analyzed is insufficient for thermal maturation. Biogenic gas generation demonstrates potential for significant natural gas accumulations even in areas where sediments have not been deeply buried.

Of the sediments cored at Site 262, trough fill and lower flank sediments had the highest levels of organic carbon. A decrease in TOC with subbottom

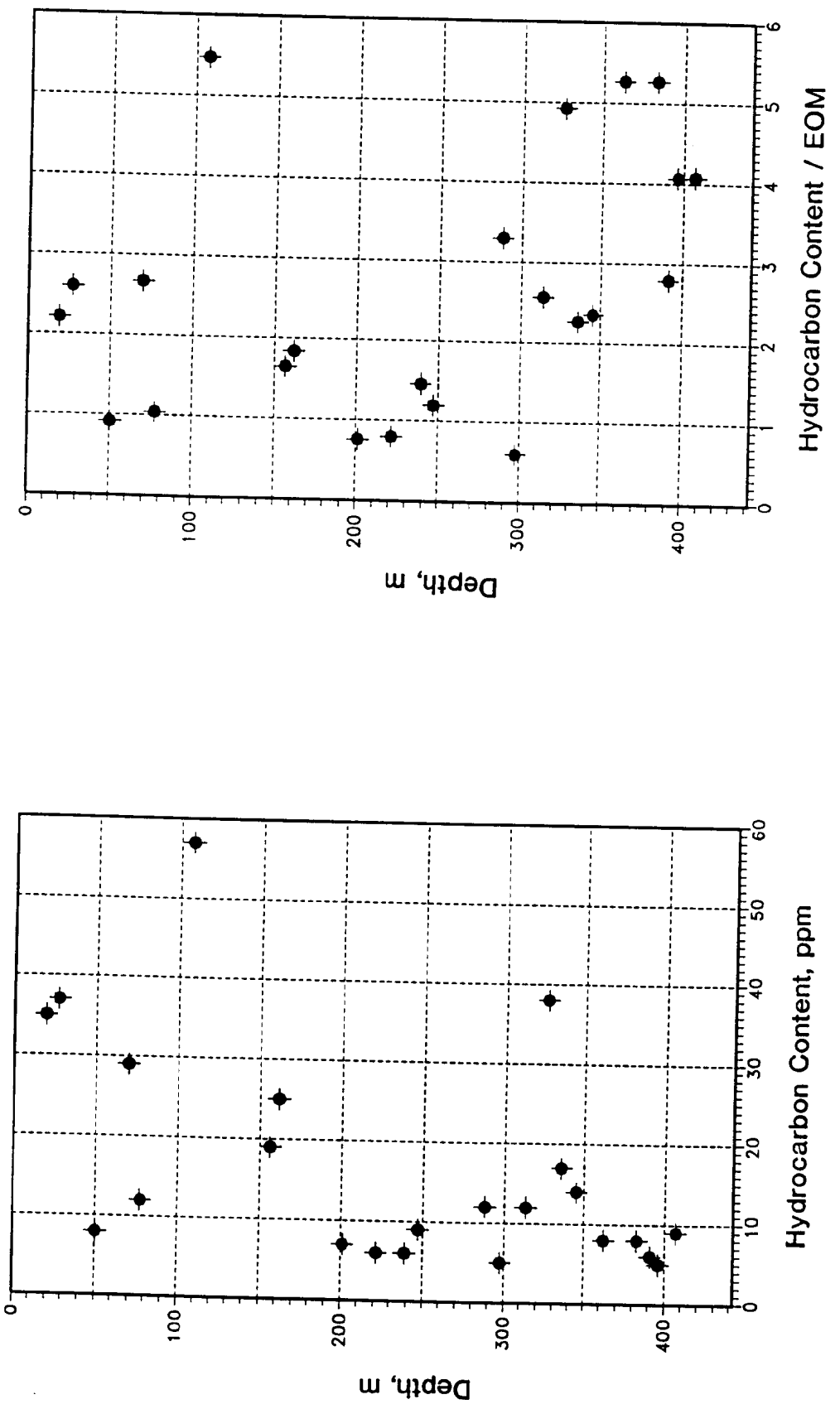

Figure 17. HYDROCARBON CONTENT OF EXTRACTS, DSDP SITE 262

Data from McKirdy and Cook, 1980

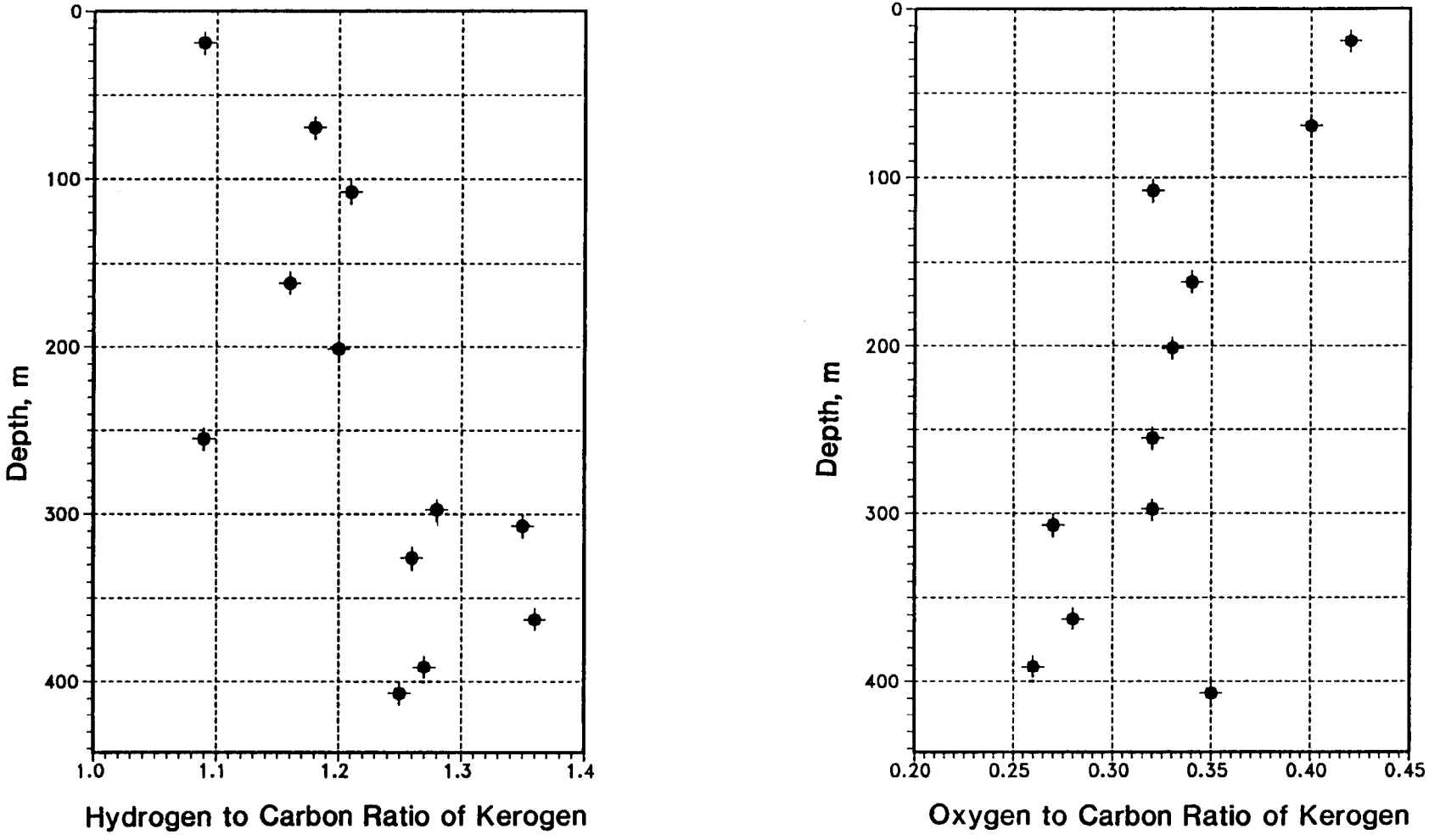

Figure 18. KEROGEN COMPOSITION, DSDP SITE 262 SEDIMENTS

Data from McKirdy and Cook, 1980

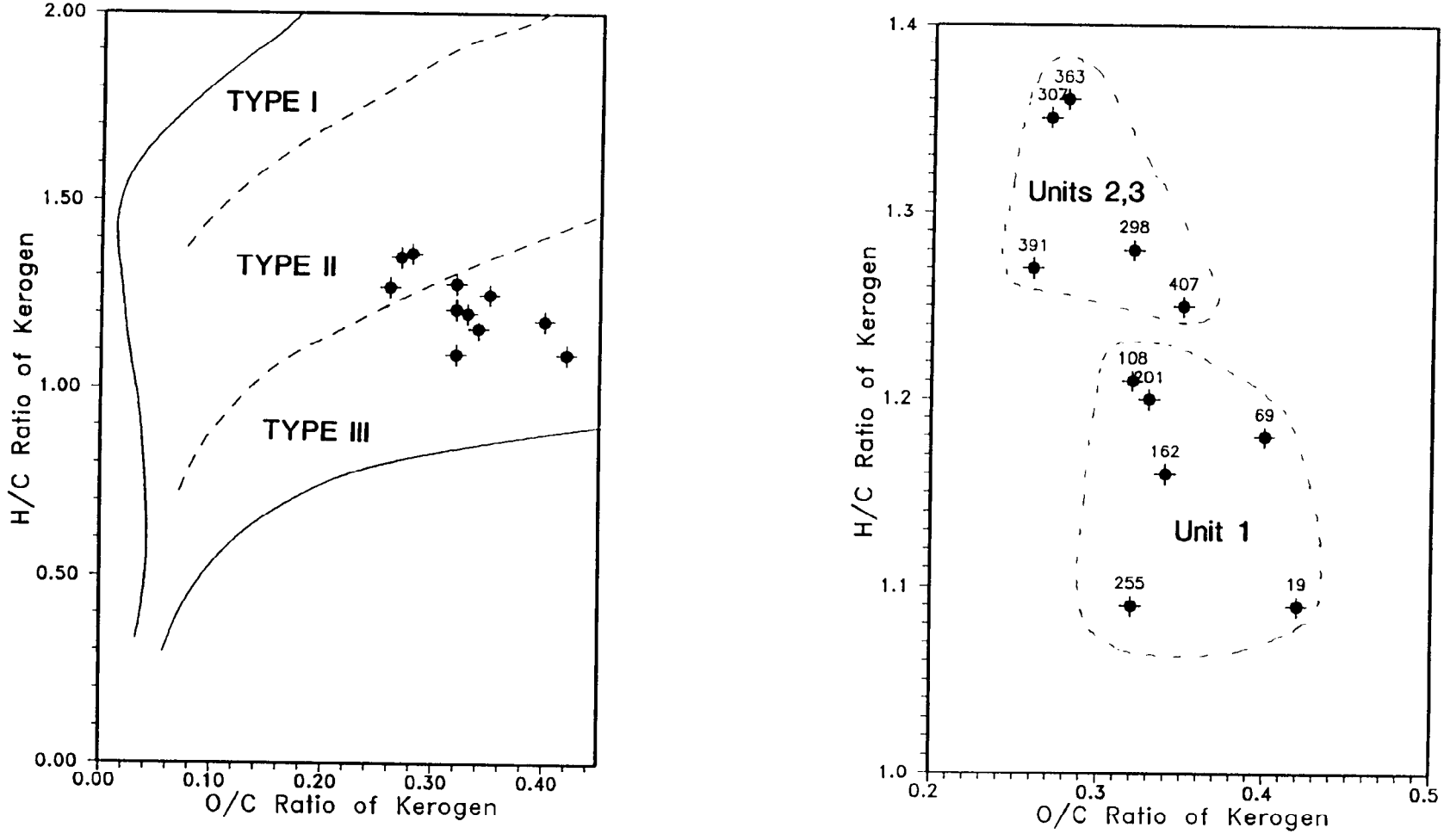

Figure 19. **VAN KREVELEN DIAGRAM OF DSDP SITE 262 KEROGEN**

Data from McKirdy and Cook, 1974; Kerogen Types from Tissot and Welte, 1984

depth suggests that sediments buried sufficiently deep to have generated hydrocarbons by thermal processes may not have adequate organic carbon. However, continental shelf strata and sub-unconformity basins on the present continental shelf of Australia have prolific oil and gas production. This indicates that some of the rocks on the descending continental plate may be petroliferous. Karig et al. (1987) have shown that large thrust sheets of continental margin sediments are being offscraped from the subducting plate and accreted to the north flank of the Timor Trough. Based on the oil and gas discovered on the adjacent continental shelf of Australia, it is likely that some mature source rocks have been accreted to the Timor Trough inner slope. Additional burial by the stacking of imbricate thrust sheets visible on seismic lines could mature the continental margin sediments, along with the trough and lower slope sediments shown at DSDP Site 262 to have adequate TOC for hydrocarbon generation. Thus thermogenic hydrocarbons may be expected in the hydrate stability zone above migration pathways in fractures and faults systems on both slopes of the Timor Trough.

PART II

GAS HYDRATES

Gas hydrates have not been recovered from sediments of the Timor Trough. Abundant methane gas was released from the sediments cored at DSDP Site 262 (Veevers et al., 1974; McIver, 1974). Pore-water geochemical anomalies led McKirdy and Cook (1980) to propose that gas hydrates were present in sediments at Site 262. No seismic evidence of gas hydrates in the Timor Trough has been mentioned in the literature.

Our analysis indicates that gas hydrates are present in sediments of the Timor Trough, but not necessarily at Site 262. The amounts of gas released from Site 262 was not sufficient to confirm hydrate presence. The geochemical anomalies attributed by McKirdy and Cook (1980) to gas hydrate presence are more likely due to sedimentary diagenetic processes. Our search of the public domain seismic lines from the Timor Trough revealed well-defined bottom simulating reflectors (BSRs) on several lines. The BSRs are typically formed on the inner (north) slope of the trough. BSRs have been noted on seismic lines from water depths of 1,000 to 1,900 m. The BSRs are more prevalent on the southeast portions of the trench. Poor coverage of the Timor Trough by public domain seismic lines makes estimates of the areal extent of BSRs speculative.

Evidence of hydrates from cores.

The only core drilling yet performed on the Timor Trough has not recovered gas hydrates. However, the Timor Trough was drilled before Deep Sea Drilling Project personnel were specifically trained in identification of hydrates in cores. Thus hydrates may have existed but gone undetected. Methane gas was released from some cores recovered from the Timor Trough. Additionally, some cores expanded due to release of methane to the extent that they were partially extruded from core liners. These features have since come to be associated with gas hydrate presence. An extensive geochemical analysis program was performed on sediments and pore water from DSDP Site 262 cores. Anomalies in the geochemical data could conceivable indicate hydrate presence.

Methane presence

Deep Sea Drilling Project (DSDP) Site 262 was drilled near the axis of the Timor Trough. Calcareous Pliocene to Holocene sediments were penetrated to a subbottom depth of 442 m. Methane was released from cores from subbottom depths of 5 to 300 m subbottom. Cores from that interval degassed vigorously

upon recovery. Gas voids were noted in the core description of Veevers et al. (1974).

Presence of large amounts of methane in recovered cores indicates the possibility of hydrate presence, but does not confirm hydrate presence. The high hydrostatic pressure exerted by the 2,300 m water column at Site 262 increases solubility of methane in the pore water relative to surface conditions. Thus, the gas released from cores on the deck of the drilling vessel may have been methane which had been dissolved in pore water, rather than gas in hydrates.

To serve as definitive proof of hydrate presence, the amount of methane released from cores must exceed that soluble in pore water at in situ conditions. Any methane in excess of pore-water solubility limit exists as either free gas or gas hydrate. If the pressure and temperature conditions are sufficient for hydrate stability, then the excess methane is present as methane hydrate, under lower pressure or higher temperature conditions the excess methane is present as free gas. The high pressures (230 - 280 atm) and low temperatures (3° - 16°C) at Site 262 indicate that methane in excess of the prevailing solubility limit would be present in the sediment interstices as hydrate.

Determination of the approximate methane solubility at in situ conditions is problematic. As reviewed by Finley and Krason (1989b), literature values for methane solubilities at typical pressures and temperatures found in subsea sediments are in wide disagreement. However, the solubility model presented by Finley and Krason (1989b) can be used to estimate solubility at the in-situ pressure and temperature conditions prevailing at Site 262.

The graph in Figure 20 summarizes the results of modeling the methane solubility at Site 262. The line in Figure 20 indicates the maximum amount of methane that the pore water can contain in solution. The graph shows that methane solubility increases with depth from 56 mM/L at the seafloor to 137 mM/L at the bottom of the hole at 442 m subbottom. Methane at or less than the indicated solubility for a given depth will be present in situ as dissolved methane. Adding methane in excess of the prevailing solubility (Figure 20) to the pore water will form hydrate.

Also shown in Figure 20 are the methane concentrations measured by McIver (1974) from canned samples of sediments from Site 262 cores. The samples range in methane content from 0.7 to 8.7 mM/L. Comparison with the solubility line in Figure 20 shows that the methane concentrations measured by McIver (1974) are 1% to 12% of the minimum amount needed to form methane hydrate at the prevailing pressure and temperature. McIver (1974) noted that the reported methane content Site 262 sediments may understate the amount of methane present at in situ conditions. Since some amount of time is needed to retrieve the core, open the core liner, and take and seal the sample, some methane would have been lost to the atmosphere prior to sampling. However, McIver (1974) did not have an estimate of the probable accuracy of the concentrations he reported.

The shipboard scientific party described substantial expansion of the cores due to core degassing. The core description indicated expansion of up to 26% on some cores, with an average of about 12%. The expansion may be due to gas

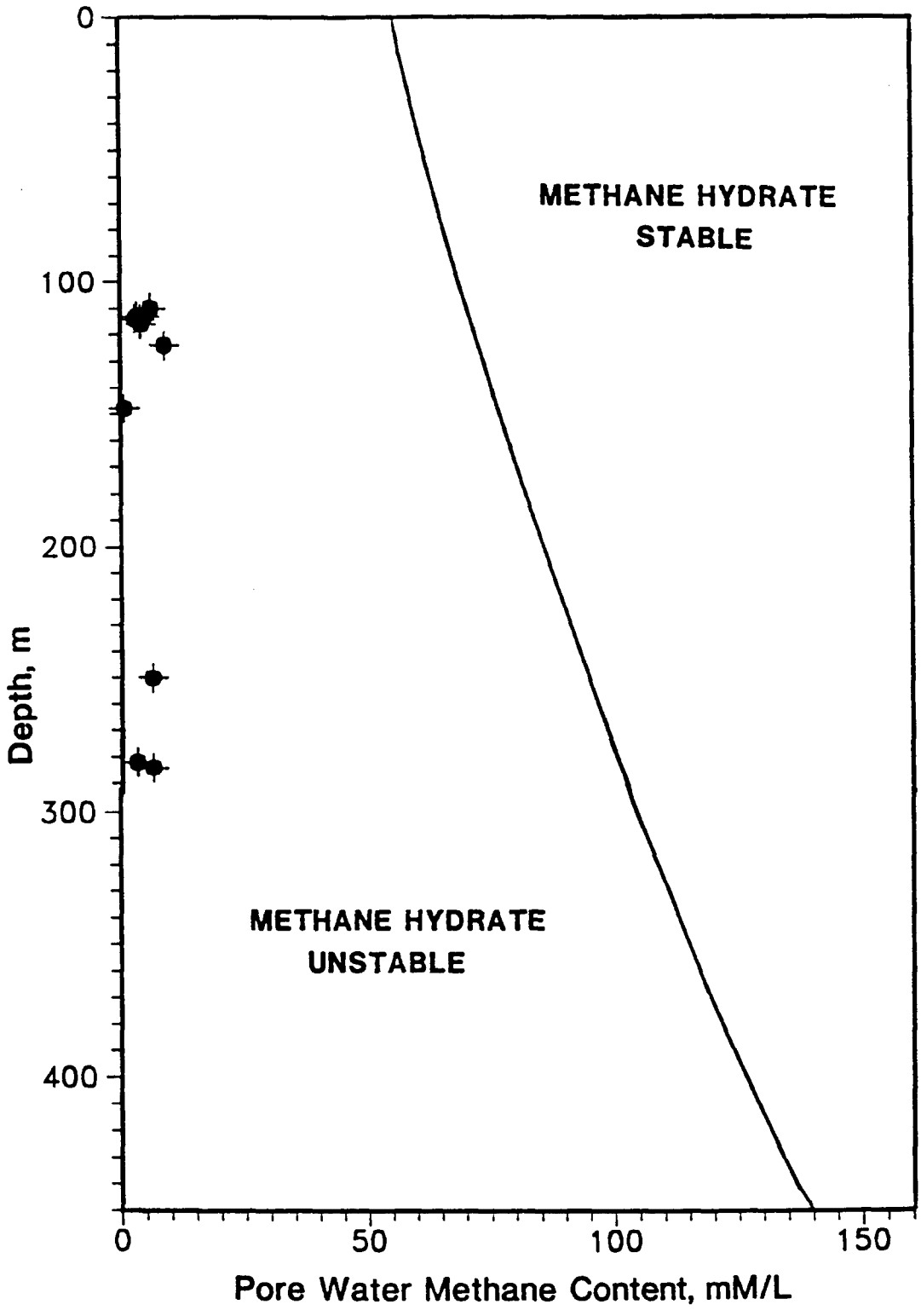

Figure 20. METHANE CONTENT AND IN-SITU METHANE SOLUBILITY, DSDP SITE 262

Solubility Curve from Finley and Krason, 1989b
Data from McIver, 1974

from dissociating hydrates or from exsolution of gas dissolved in pore water. The methane dissociation model shown in Figure 20 can be used to determine if the 25% gas expansion documented from Site 262 cores was sufficient to indicate hydrate presence.

The maximum expansion of a core that could be attributed to exsolution of methane from pore water in the absence of hydrates was calculated from the methane solubility data graphed in Figure 20. The volumetric solubility of methane in the pore water was obtained by multiplying the solubility data in millimoles of methane per liter of water by .0224 liters per millimole. The solubility of methane at Site 262 pressure and temperature conditions was converted from liters of methane per liter of pore water to liters of methane per liter of sediment by multiplying by porosity. The porosity of the Site 262 sediments was determined from a least-squares fit of the bulk density data reported by Rocker (1974) using the equation:

$$porosity = (bulk\ density - grain\ density) / (1 - grain\ density).$$

The maximum expansion of the cores from Site 262 attributable solely to dissolved methane in the pore water is shown by the curve in Figure 21. Core expansion of 80% at the surface to about 115% at total depth could be explained by exsolution of dissolved methane in the absence of hydrates.

Accurate volumetric estimates of gas release from Site 262 cores were not reported by Veevers et al. (1974). However, the core description and photographs from the site report document voids in the recovered cores. At least some of the voids in the core may be due to gas exsolution and/or hydrate decomposition. The reported void space expressed as percentage of the core volume is also plotted in Figure 21. Extrusion of the core material was measured on cores 8 through 15 (62 - 138 m). The extruded core expressed as percentage of the core length is also graphed in Figure 21. While it is probable that neither estimate accurately measures total expansion of the core caused by gas presence, each is less than the maximum expansion which could occur by exsolution of dissolved methane. Thus the documented core expansion at Site 262 is insufficient to definitively indicate hydrate presence.

Geochemical Anomalies

McKirdy and Cook (1980) proposed that apparent anomalies in the geochemistry of the pore water at DSDP Site 262 could be reconciled if gas hydrates existed in the sediments. Their interpretation of the pore water chemistry data of Cook (1974) hinged on geochemical evidence of vertical diffusion of pore water components. Salinity of the Site 262 pore water increased with depth, particularly from 240 m to 442 m (Figure 22, Table 1). Veevers et al. (1974) and Cook (1974) interpreted the salinity profile at Site 262 to be due to upward diffusion of ions from an underlying salt source. However, McKirdy and Cook (1980) proposed that the trends in alkalinity and sulfate values of the pore water were "fossil profiles" which could only have existed in the absence of diffusion, particularly in the upper 300 m of sediment. To accommodate the two divergent interpretations, McKirdy and Cook (1980) proposed that gas hydrates were present in abundance in the upper 300 m of sediment. McKirdy and Cook (1980) stated that the pro-

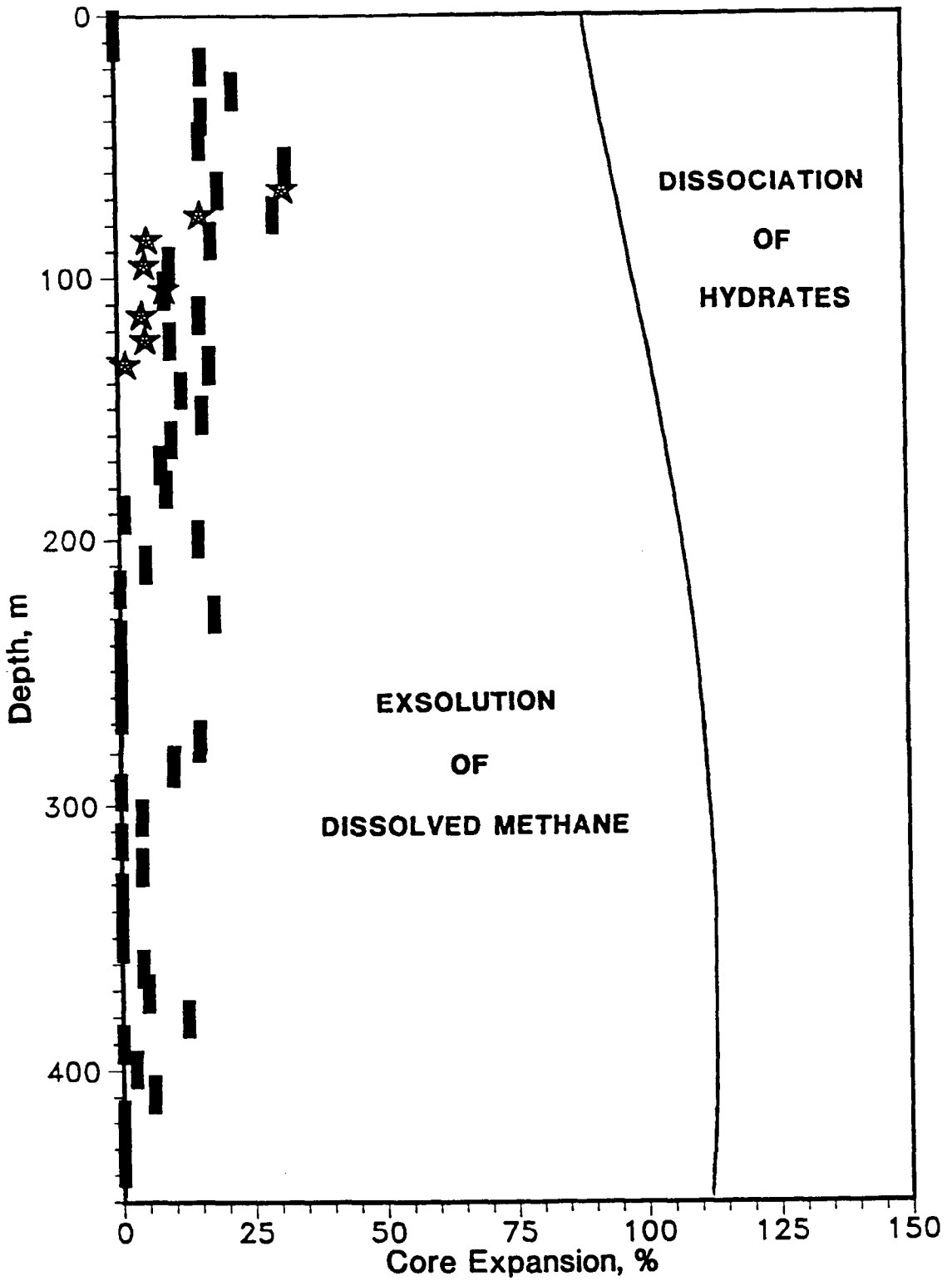

Figure 21.

CORE EXPANSION AS INDICATOR OF HYDRATE PRESENCE, DSDP SITE 262, TIMOR TROUGH

Data from Veevers et al., 1974: (▮) Core Void Space, (★) Core Extrusion
Methane Hydrate Fields from Finley and Krason, 1989b

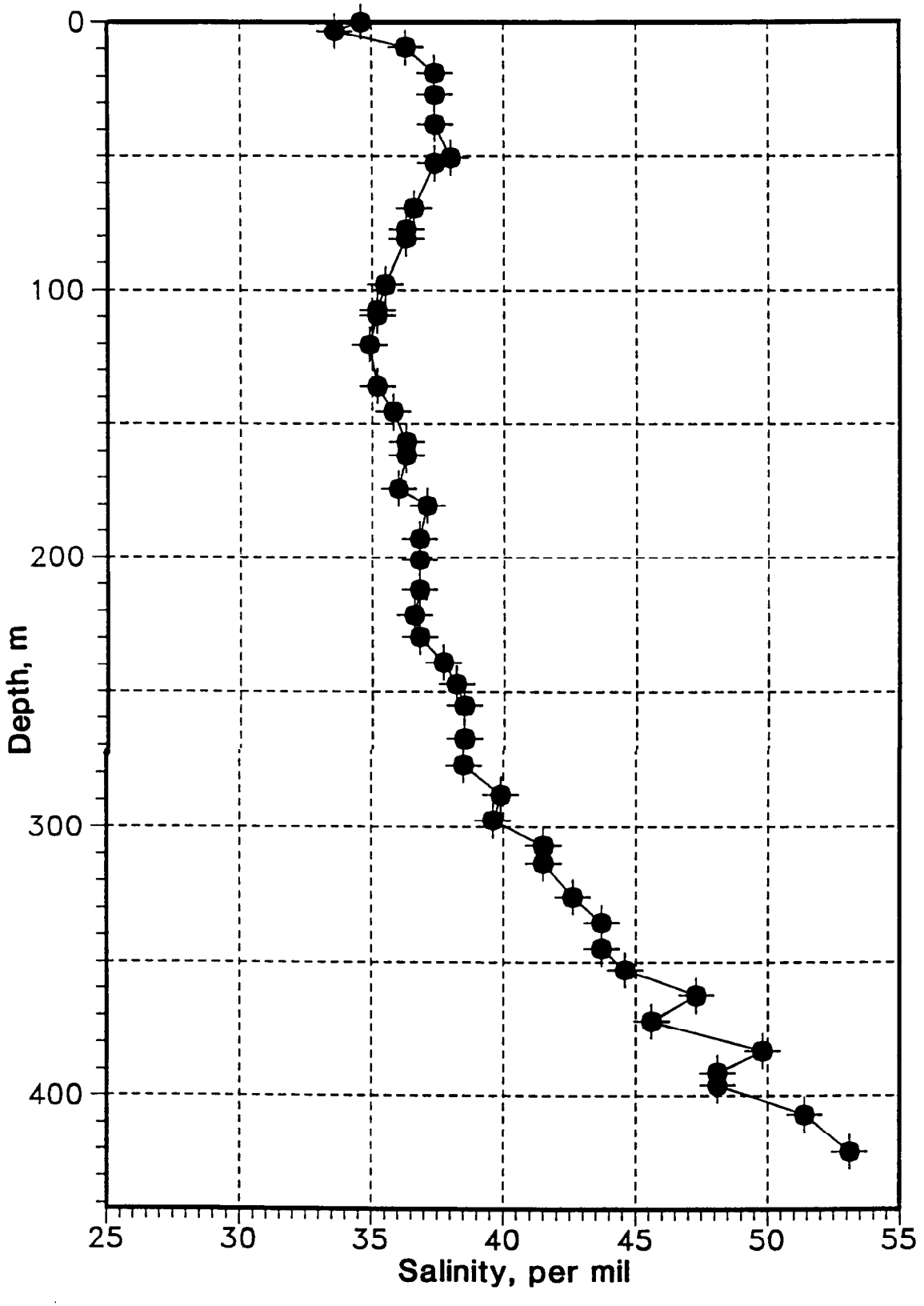

Figure 22. PORE WATER SALINITY, DSDP SITE 262

posed hydrate "Reduces the effective permeability to zero, thus blocking fluid migration in the top 300 m of the sediment."

Active diffusion of salt was the first assumption that McKirdy and Cook (1980) used to eventually infer hydrate presence at Site 262. Salinity profiles similar to that from Site 262 (Figure 22) have also been measured in the Gulf of Mexico at DSDP Sites 2, 88, 89, and 92 (Manheim et al. 1973). Sites 2 and 92 were drilled directly over salt diapirs. Sites 88 and 89 were drilled in the Mexican Ridges geological province, were underlying shale diapirs and possibly by salt diapirs have transported ions toward the surface. A direct relationship is seen in the Gulf of Mexico drillholes between interstitial salinity and proximity to salt bodies. Veevers et al. (1974), Cook (1974), and McKirdy and Cook (1980) stated that the salinity profile at Site 262 in the Timor Trough is best explained as a product of diffusion from underlying salt. The Gulf of Mexico pore water salinity data corroborate that interpretation. The salinity profile at Site 262 may also be due to active vertical migration of pore water in addition to simple diffusion of pore water components.

The static nature of pore water constituents, as evidenced by the alkalinity and sulfate profiles, was the second principal component of the interpretation of hydrate presence at Site 262 by McKirdy and Cook (1980). The combination of high alkalinity and low sulfate concentrations in pore water (Figure 23) and abundant methane in cores between 10 m and 300 m subbottom depth at Site 262 is indicative of active microbial methanogenesis (Claypool and Kaplan, 1974). The isotopic signature of the methane released from Site 262 cores was reported by Claypool and Kvenvolden (1983) to range between $\delta^{13}C$ = -77.0 per mil and $\delta^{13}C$ = -58.6 per mil, convincingly demonstrating its bacterial origin. McKirdy and Cook (1980) concurred that the methane present in Site 262 cores was generated by biogenic processes as outlined by Claypool and Kaplan (1974), but concluded that the alkalinity and sulfate levels recorded at Site 262 could not have been caused by ongoing bacterial processes deep in the sedimentary section. The alkalinity and sulfate content of deeper sediments were relics of microbial processes operant within the 5 - 10 m surficial sediment interval. Since distinct trends and inflections exist in the sulfate and alkalinity profiles between 10 m and 300 m subbottom (Figure 23), McKirdy and Cook (1980) stated that diffusion was not operant above 300 m. They reconciled their interpretations of no diffusion in gassy sediments above 300 m subbottom depth with obvious diffusion in deeper sediments by invoking hydrate presence in the upper section.

The abundant methane in Site 262 sediments may indicate hydrates. However, we disagree with McKirdy and Cook (1980) that the pore water geochemistry of Site 262 is necessarily a product of hydrate formation. Cook (1974) and McKirdy and Cook (1980) postulated that the alkalinity and sulfate profiles at Site 262 could be indicative of two scenarios:

1. Present-day biogenic activity occurring to a depth of 300 m
2. Biogenic activity limited to the upper 5-10 m of sediment with preservation of past levels of metabolites and products with burial.

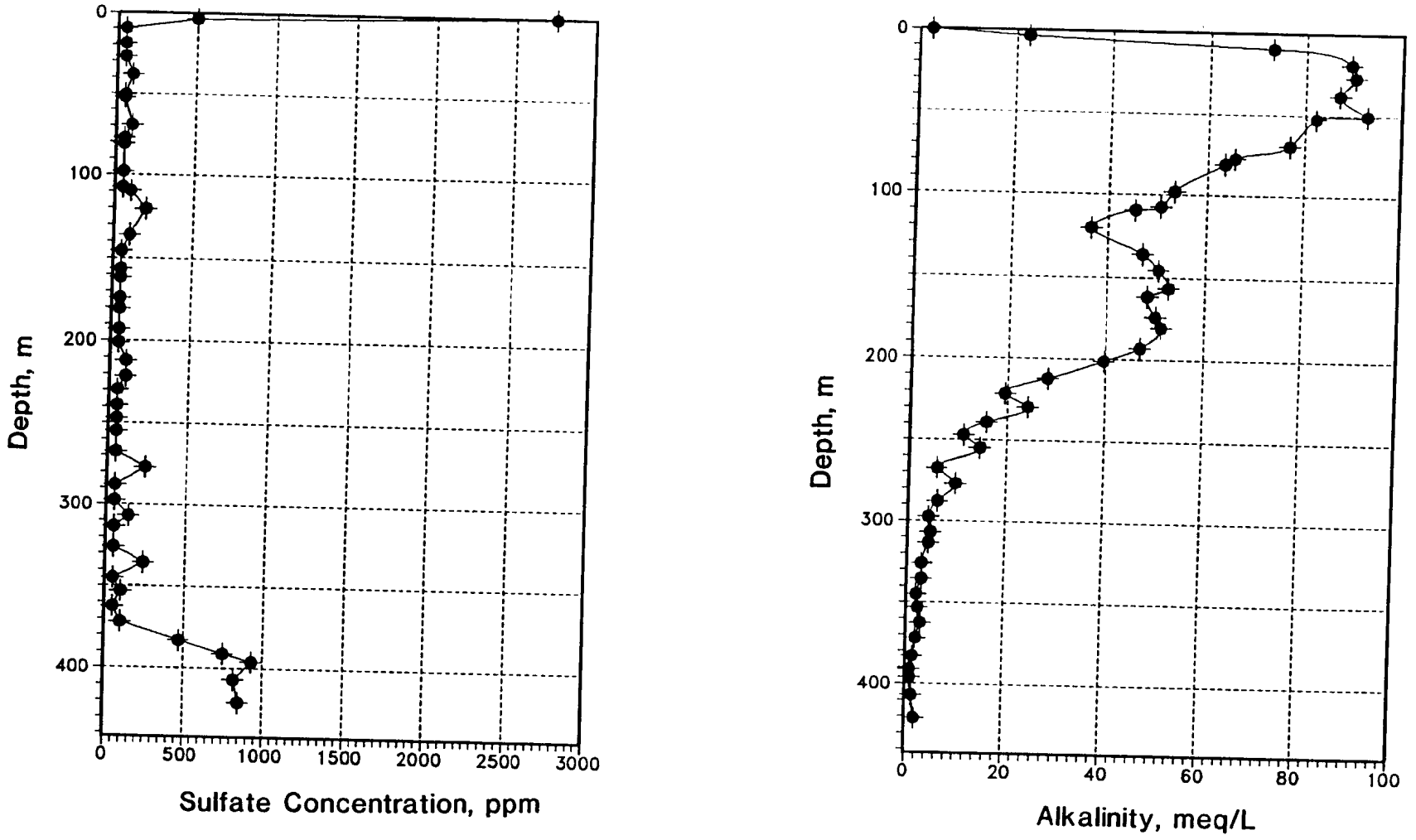

Figure 23.

PORE WATER SULFATE CONTENT AND ALKALINITY, DSDP SITE 262

Data from Cook, 1974

Cook (1974) preferred the second interpretation, but did not preclude active microbial activity throughout the sediment column. However, McKirdy and Cook (1980) rejected microbial activity throughout the sediment column, and invoked hydrate presence to make the Site 262 data fit into the scenario of "fossil profiles". Our analysis of the pore water geochemical data from Site 262 indicates that interpretation (1) is more probable, that the alkalinity and sulfate profiles are the product of continuous bacterial methanogenesis downhole.

The high alkalinity levels at shallow depths at Site 262 largely result from sulfate reducing bacteria converting organic matter to CO_2 which is present as bicarbonate (HCO_3^-) in pore water. Additional bicarbonate is added to pore water subsequent to sulfate reduction by anaerobic bacterial fermentation of organic matter. The down-hole decrease in alkalinity is principally caused by reduction of CO_2 to methane by anaerobic methanogenic bacteria. The alkalinity profile of Site 262 (Figure 23) is typical of that found in organic rich marine sediments (Claypool and Kaplan, 1974; Claypool and Kvenvolden, 1983). The alkalinity and sulfate profiles at Site 262 indicate a sulfate reducing zone between the sea floor and about 8 m depth. Beneath the sulfate reducing zone, an active microbial population converts organic matter to CO_2, and CO_2 to methane. The zone of active bacterial methanogenesis appears to extend to about 300 m. Bacterial activity in deeper sediments may be limited by the paucity of organic carbon at depth (Figure 15).

McKirdy and Cook (1980) claimed that present-day bacterial activity at depths of greater than 10 m were precluded because the abundant methane in Site 262 sediment could not exist in the presence of sulfate reducing bacteria. We contend that sulfate reduction is essentially complete by a sediment depth of 9.5 m. Many studies have shown that methane rarely attains high concentrations in the presence of sulfate (Berner, 1980; Claypool and Kaplan, 1974; Claypool and Kvenvolden, 1983). However, the sulfate profile from Site 262 indicates that high sulfate levels only exist at the seafloor (2,800 ppm) and at 3.5 m (500 ppm) (Figure 23, Table 1). By a depth of 9.5 m, the sulfate level has reached a 50 ppm baseline. From 9.5 m to 370 m the sulfate concentration fluctuates between 50 and 100 ppm with three small peaks at 120 m (200 ppm), 277 m (240 ppm), and 336 m (240 ppm). From a depth of 383 m to the bottom of the hole the sulfate concentration in pore water is elevated, presumably by diffusion from the postulated underlying evaporite. Nikaido (1977) demonstrated that methane generation proceeds once sulfate levels fall below 560 ppm. High rates of methanogenesis were noted by Nikaido (1977) at sulfate concentrations between 100 ppm and 430 ppm. The sulfate levels in Site 262 cores from depths of between 9.5 m and 372 m averages 76 ppm. Thus, the sulfate levels in that depth range at Site 262 are sufficiently depleted to allow bacterial methanogenesis throughout the section.

McKirdy and Cook (1980) apparently contended that alkalinity of pore water changes only within the sulfate reduction zone. Since the sulfate reduction zone occurs only within the upper 5 to 8 m of sediments, they concluded that the present alkalinity profile indicates the alkalinity levels prevailing in the sediment when the sediment exited from the zone of sulfate reduction. We interpret the literature on the diagenesis of organic-rich sediments (e.g. Claypool and Kaplan, 1974; Claypool and Rice, 1981; Wigley et al, 1982) to indicate that the alkalinity

profile beneath the sulfate reduction zone is the net result of many inputs and outputs. The alkalinity reflects CO_2 inherited from the zone of sulfate reduction and additional CO_2 generated from anaerobic fermentation of organic matter. Several sinks exist for CO_2 in sediments, including bacterial reduction to methane and precipitation as carbonate minerals. The alkalinity profile at Site 262 is a product of such dynamic interactions beneath the sulfate reduction zone. The trends and peaks seen between 9.5 and 300 m depth in the alkalinity profile therefore reflect present day processes, rather than being relict "fossil profiles" as indicated by McKirdy and Cook (1980). Gas hydrates were invoked by McKirdy and Cook (1980) solely to reduce permeability and therefore preserve the "fossil profiles" from dissipation by diffusion. Since the alkalinity profile at Site 262 is not a relict feature of near-surface processes, the requirement of lowered permeability, and therefore hydrate presence, is obviated. The alkalinity and sulfate trends at Site 262 are consistent with efficient bacterial methanogenesis, which in turn may result in hydrate formation. However, the pore water chemistry at Site 262 does not in and of itself indicate hydrate presence.

Seismic Evidence of Hydrates

No seismic evidence of gas hydrates in sediments of the Timor Trough has been reported in the literature. Our review of seismic lines from the study region has detected bottom simulating reflectors (BSRs) on various seismic lines.

The most visible example of a BSR on a Timor Trough seismic line is from Gulf line IBA-54 (Figure 24). The line shows the inner lower slope (toward Timor), the trough floor and the lower portion of the outer trough slope (toward Australia). The multichannel line images about 3 sec (~3,000 m) of the sediments of the descending plate and trough floor. Due to the intense deformation within the accreted thrust sheets, only about 1.5 sec (~1,500 m) of inner trough slope sediments can be resolved on line IBA-54. A BSR continues from the left-hand border of the line for about 1.5 km at a subbottom depth of about 0.5 sec (~500 m). The reflector reappears at 0.6 sec subbottom beneath the fold marking the deformation front at the contact of the inner trough slope and the trough floor. The reflector clearly cuts across the sedimentary reflectors. It also appears to have a negative polarity relative to the seafloor reflector. The subbottom depth of the BSR is within the range of depths expected for the base of the gas hydrate stability zone in view of the 3.3°C/100 m thermal gradient reported by Erickson (1974) for the Timor Trough.

A migrated section of the same seismic line is illustrated in Figure 25. The migration enhances resolution of subbottom sediment reflectors, particularly the calcareous turbidites comprising the trough floor. In the upper panel of Figure 25, the extreme vertical exaggeration impedes resolution of the BSRs from the surrounding sedimentary layers. However, the discordant relationship of sediment layers and the BSR can be for the BSR near the left border of the figure. The BSR near the deformation front is visible in lower panel of Figure 25 at a much lower vertical exaggeration. The lower panel shows distinctly the discordance of the BSR with reflectors of each limb of the anticline. Additionally the distinct BSR

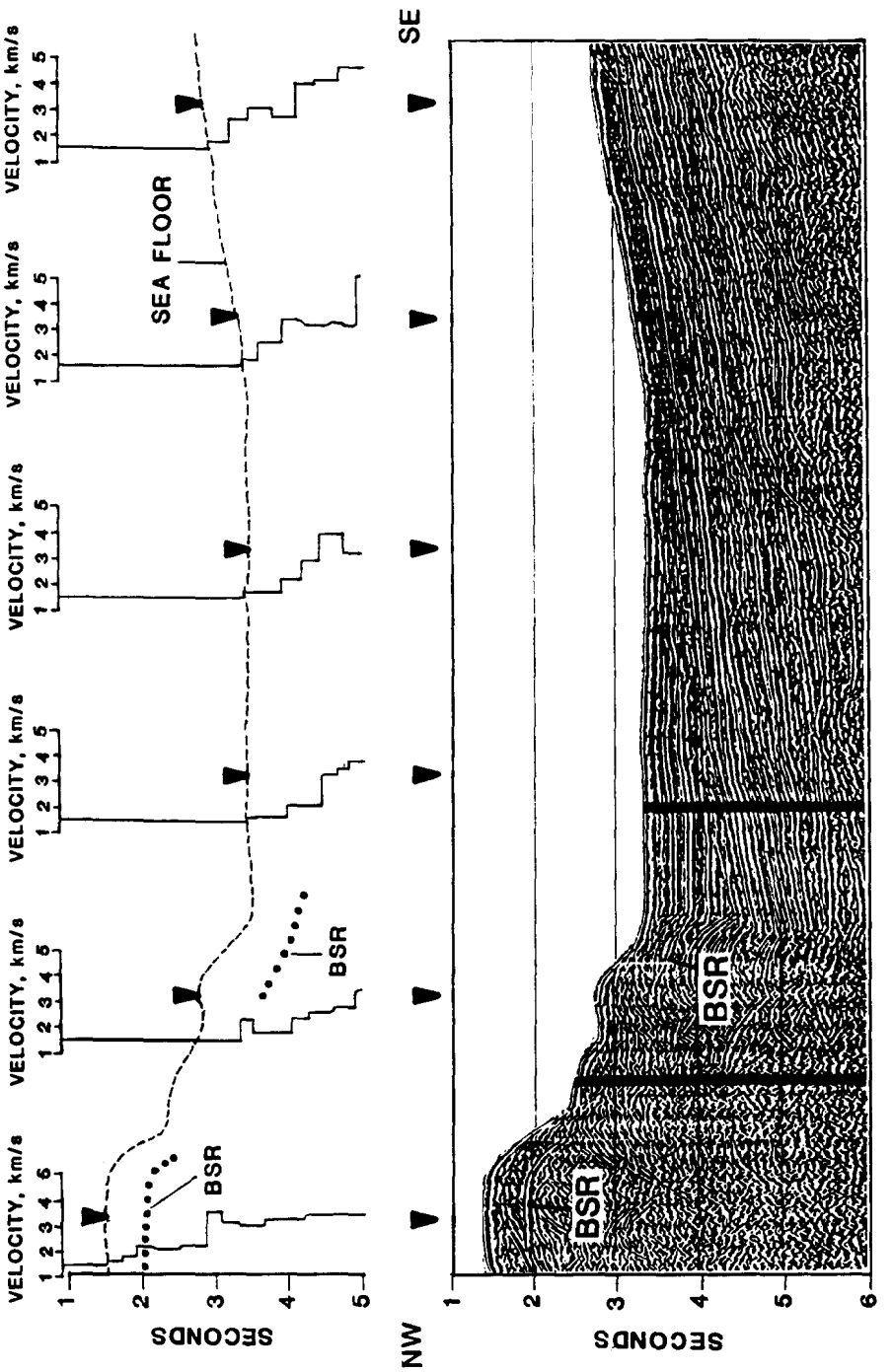

Figure 24. SEISMIC LINE IBA-54, TIMOR TROUGH

After Montecchi, 1976

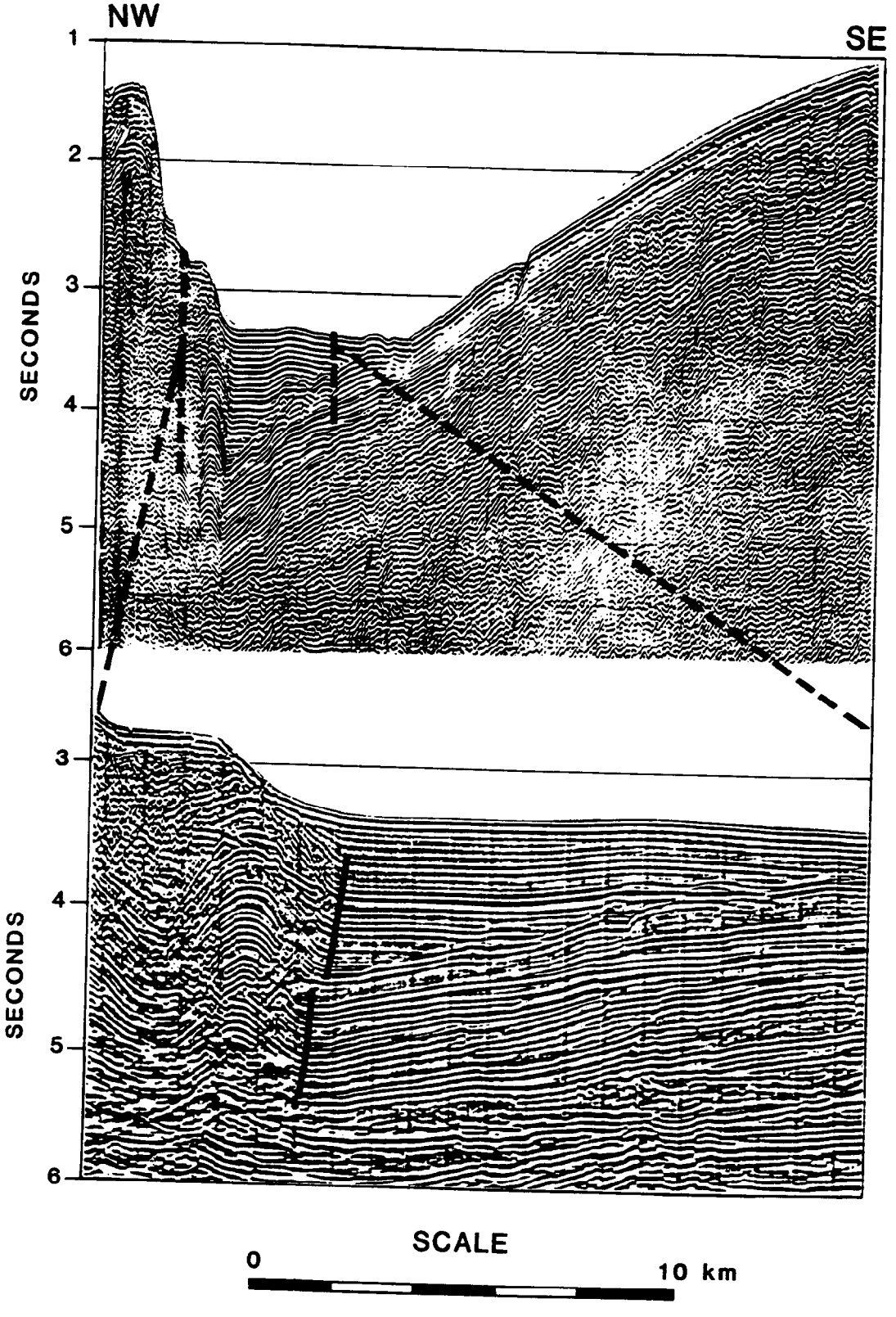

Figure 25. **MIGRATED SEISMIC LINE IBA-54, TIMOR TROUGH**

After Montecchi, 1976

can be traced into the horizontally bedded turbidites of the trough floor. The trough floor reflector which corresponds in depth to the BSR crossing the anticline is enhanced in amplitude and wavelength. This suggests that the impedance contrast which caused the BSR in the inner trough setting also exists within the trough floor sediments. The possible hydrate reflector in the trough floor sediments loses its continuity where it merges with the inclined sediments of the descending plate.

Seismic velocity analyses of the data displayed on seismic line IBA-54 shows high seismic velocity at subbottom depths corresponding to that of the BSR. On the two left-hand velocity scans in Figure 24, local velocity maxima appear to coincide with the BSRs. A velocity increase would be consistent with a hydrate origin for the BSRs, as noted by Paull and Dillon (1979). However, velocity anomalies were not found by Shipley et al. (1979) on seismic lines with BSRs from the Blake Outer Ridge, Gulf of Mexico, Colombia Basin, Panama Basin, and the Middle America Trench. Nor were velocity anomalies noted on seismic lines with vivid BSRs from the Beaufort Sea (Finley and Krason, 1989a). Diagenetic processes unrelated to hydrate formation, which could conceivably cause BSRs (Hein et al., 1978), may also cause some type of seismic velocity anomaly.

Another example of a BSR on a seismic line is shown in Figure 26. The line shot by BOCAL oil company was presented by Hamilton (1979). It shows the continental shelf and upper continental slope of Timor. The basin on the right hand side of the figure is not the trough floor, but is a slope basin caused by damming of downslope sediment transport. A BSR can be traced for about 3 km through the sediments of the basin.

We have identified BSRs on a number of seismic lines from the Timor Trough study region. In addition to lines pictured in Figures 24, 26, and 26, BSRs were found at appropriate subbottom depths is seismic lines from inner slope of the Timor Trough published by Karig et al. (1987). Bottom simulating reflectors can also be picked out on unpublished lines of the Timor Trough shot by the Bureau of Mineral Resources of Australia. The BSRs are typically concentrated in the rollover anticline of the lowermost thrust sheet of the accretionary wedge, in settings similar to that of the BSR on line IBA-54. Many high-quality lines, however, do not show BSRs, for example Figures 6 and 7.

Regionally, BSRs also occur on lines from other portion of the Banda and Sunda Arcs. We have identified BSRs on lines from the Java Trench and in numerous forearc basins, for example the Savu Basin northwest of Timor. The most consistently developed BSRs of the region are from the Seram Trough offshore of Irian Jaya (western New Guinea). The BSRs in the Seram Trough occur in a tectonic setting analogous to that of the Timor Trough. However, the BSRs of the Seram Trough are more distinct; bold BSRs are visible on all seismic lines from the Seram Trough, whereas BSRs are only sporadically apparent on lines from the Timor Trough.

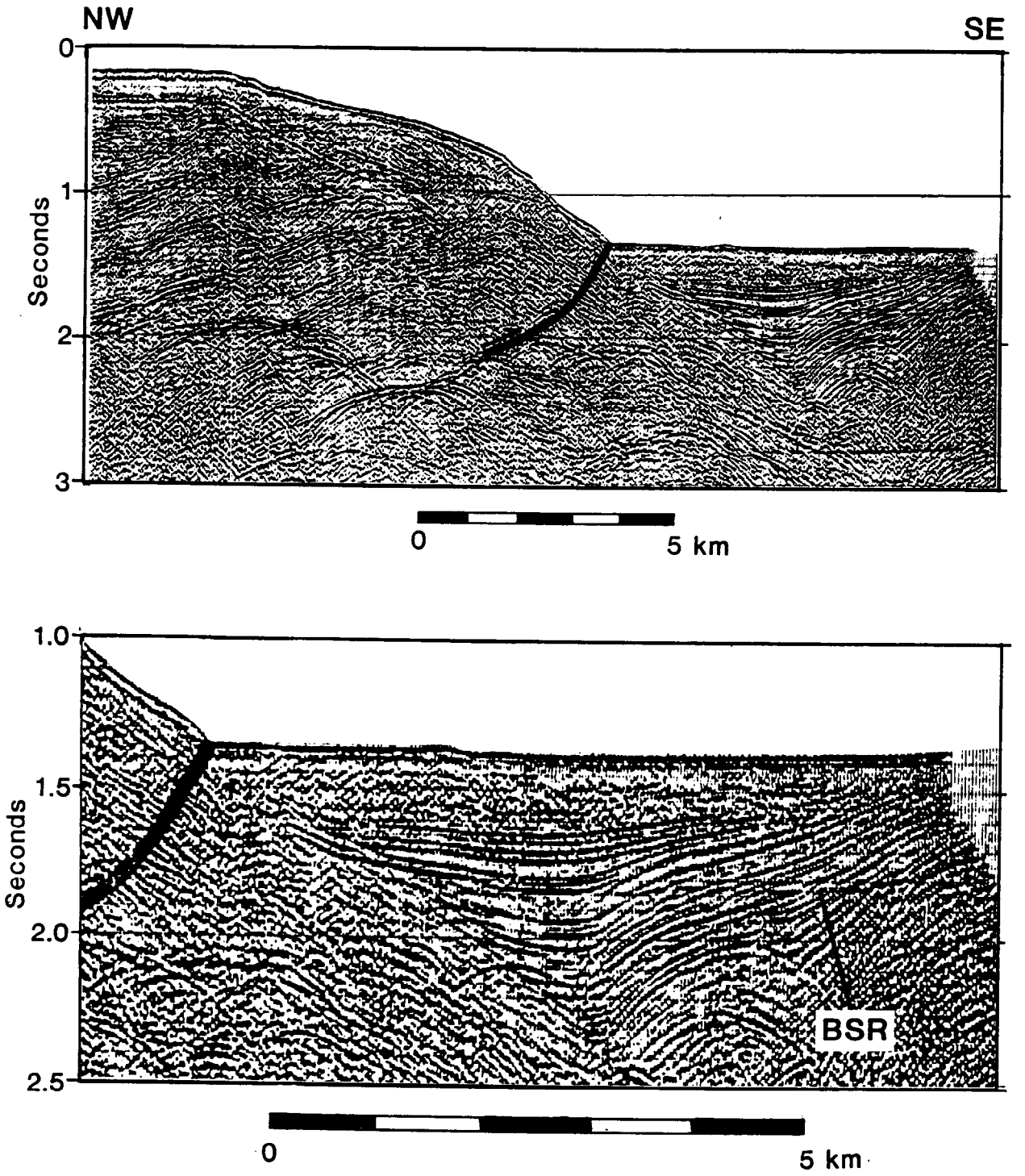

Figure 26. **SECTION OF BOCAL SEISMIC LINE THROUGH SLOPE BASIN, TIMOR TROUGH**

Approximate Location: 125° 37'E

After Hamilton, 1979

Potential Gas Resources Associated with Hydrates

With no confirmed evidence of hydrates in the Timor Trough study region potential gas estimates are speculative. Bottom simulating reflectors were detected along an area of the accretionary prism offshore of western Timor measuring about 5,000 km^2. We project that about 20% of the area is indeed underlain by BSRs, for a net areal extent of 1,000 km^2. Assuming that the impedance contrast that causes the BSRs is due to hydrate filling 50% of the pore space of a 40% porosity sediment, a 1 m thick layer of hydrate-impregnated sediment would contain 2×10^8 m^3 of hydrate. Using a volumetric conversion factor of 150 m^3 gas per m^3 hydrate, about 3×10^{10} m^3 or 1 trillion cubic feet (tcf) may be present as hydrates. If the possible hydrate layer causing the BSRs is thicker, proportionally more gas would be present. Thus a 10 m thick layer of 40% porosity sediment with 50% of the pore space filled with hydrate would contain 3×10^{11} m^3 or 10 tcf of gas.

The BSRs of the Timor Trough study region often correspond to anticlines with a bathymetric expression (Figure 24). This mode of occurrence is conducive to trapping free gas beneath the hydrate layer. We have numerically analyzed the bathymetric surfaces shown in Figure 1 to determine the possible volume of gas traps formed from hydrates. Using methodology discussed in Finley and Krason (1989a, 1989b), we have identified bathymetric highs on the accretionary prism offshore of Timor capable of containing about 10^{10} m^3 or 0.3 tcf of gas in sub-hydrate traps. There is no evidence as to whether any of the potential sub-hydrate gas traps are presently occupied.

REFERENCES

Audley-Charles, M.G., 1968, The geology of Portuguese Timor: Geological Society of London Memoir 4, 76 p.

Beck, R.H., and Lehner, P., 1974, Oceans, new frontier in exploration: American Association of Petroleum Geology Bulletin, v. 58, p. 376-395.

Berner, 1980, Early diagenesis: a theoretical approach: Princeton University Press, 241 p.

Bode, G.W., 1974, Carbon and carbonate analyses, leg 27, *in* Veevers, J.J., and Heirtzler, J.R., et al., Initial Reports of the Deep Sea Drilling Project, v. 27: U.S. Government Printing Office, Washington, p. 499-502.

Bowin, C., Purdy, G.M., Johnston, C., Shor, G., Lawver, L., Hartono, H.M., and Jezek, P., 1980, Arc-continent collision in Banda Sea Region: American Association of Petroleum Geologists Bulletin, v. 64, p. 868-915.

Charlton, T.R., 1989, Stratigraphic correlation across an arc-continent collision zone: Timor and the Australian northwest shelf: Australian Journal of Earth Sciences, v. 36, p. 263-274.

Claypool, G.E., and Kaplan, I.R., 1974, The origin and distribution of methane in marine sediments, *in* Kaplan, I.R., (ed.), Natural gases in marine sediments: New York, Plenum, p. 94-129.

Claypool, G.E., and Kvenvolden, K.A., 1983, Methane and other hydrocarbon gases in marine sediment: Annual Reviews of Earth and Planetary Sciences, V. 11, p. 299-327.

Cook, H.E., Zemmela, I., and Matti, J.C., 1974, X-ray mineralogical data, eastern Indian Ocean–Leg 27, Deep Sea Drilling Project, *in* Veevers, J.J., and Heirtzler, J.R., et al., Initial Reports of the Deep Sea Drilling Project, v. 27: U.S. Government Printing Office, Washington, p. 535-548.

Cook, P.J., 1974, Geochemistry and diagenesis of interstitial fluids and associated calcareous oozes, Deep Sea Drilling Project, Leg 27, Timor Trough, *in* Veevers, J.J., and Heirtzler, J.R., et al., Initial Reports of the Deep Sea Drilling Project, v. 27: U.S. Government Printing Office, Washington, p. 463-480.

Crostella, A., and Powell, D.E., 1976, Geology and hydrocarbon prospects of the Timor Area: Indonesian Petroleum Association Proceedings, v. 4, p. 149-171.

Erickson, A.J., 1974, Leg 27 heat-flow data, *in* Veevers, J.J., and Heirtzler, J.R., et al., Initial Reports of the Deep Sea Drilling Project, v. 27: U.S. Government Printing Office, Washington, p. 207-210.

Finley, P.D., and Krason, J., 1989a, Basin analysis, formation and stability of gas hydrates of the Beaufort Sea: U.S. Department of Energy, DOE/MC/21181-1950, v. 12, 243 p.

Finley, P.D., and Krason, J., 1989b, Summary report: evaluation of the geological relations to gas hydrate formation and stability: U.S. Department of Energy, DOE/MC/21181-1950, v. 15, 43 p.

Hamilton, W., 1979 Tectonics of the Indonesian Region: U.S. Geological Survey Professional Paper 1078, 345 p.

Hein, J.R., Scholl, D.W., Barron, J.A., Jones, M.G., and Miller, S., 1978, Diagenesis of late Cenozoic diatomaceous deposits and formation of the bottom simulating reflector in the southern Bering Sea: Sedimentology, V. 25, p. 155-181.

Johnston, C.R., and Bowin, C.O.. 1981, Crustal reactions resulting from the mid-Pliocene to Recent continent-island arc collision in the Timor region: Bureau of Mineral Resources, Australian Geology and geophysics Journal, v. 6, p. 223-243.

Karig, D.E., Barber, A.J, Charlton, T.R., Klemperer, S., and Hussong, D.M., 1987, Nature and distribution of deformation across the Banda Arc-Australian Collision zone at Timor: Geological Society of America Bulletin, v. 98, p. 18-32.

Manheim, F.T., Sayles, F.L., and Waterman, L.S., 1973, Interstitial water studies on small core samples, Deep Sea Drilling Project Leg 10, *in* Initial Reports of the Deep Sea Drilling Project, v. 10: U.S. Government Printing Office, Washington, p. 615-623.

McIver, R.D., 1974, Methane in canned core samples from Site 262, Timor Trough, *in* Veevers, J.J., and Heirtzler, J.R., et al., Initial Reports of the Deep Sea Drilling Project, v. 27: U.S. Government Printing Office, Washington, p. 453-454.

McKirdy, D.M., and Cook, P.J., 1980, Organic geochemistry of Pliocene-Pleistocene calcareous sediments, DSDP Site 262, Timor Trough: American Association of Petroleum Geologists Bulletin, v. 64, p. 2118-2138.

Milson T.D., and Audley-Charles, M.G., 1986, Collision of Australia and Indonesia, *in* Coward, M.P., and Ries, A.C., eds, Collision Tectonics, Geological Survey (London), Special Publication n 19.,

Montecchi, P.A., 1976, Some shallow tectonic consequences of subduction and their meaning to the hydrocarbon explorationist, *in* Circum-Pacific energy and mineral resources: American Association of Petroleum Geologists Memoir 25, p. 189-202.

Park, R.G., 1987, Geological Structures and Moving Plates: Chapman and Hall, New York, 336 p.

Paull, C.K., and Dillon, W.P., 1979, Appearance and distribution of the gas hydrate reflection in the Blake Ridge region, offshore southeastern United States: U.S. Geological Survey Miscellaneous Field Studies Map MF-1252.

Rice, D.D., and Claypool, G.E., 1981, Generation, accumulation, and resource potential of biogenic gas: American Association of Petroleum Geologists, v. 65, p. 5-24.

Robinson, P.T., Thayer, P.A., Cook, P.J., and McKnight, B.K., 1974, Lithology of Mesozoic and Cenozoic sediments of the eastern Indian Ocean, Leg 27, Deep Sea Drilling Project, *in* Veevers, J.J., and Heirtzler, J.R., et al., Initial Reports of the Deep Sea Drilling Project, v. 27: U.S. Government Printing Office, Washington, p. 1001-1048.

Rocker, K., 1974, Physical properties measurements and test procedures for Leg 27, *in* Veevers, J.J., and Heirtzler, J.R., et al., Initial Reports of the Deep Sea Drilling Project, v. 27: U.S. Government Printing Office, Washington, p. 433-444.

Shipley, T.H., Houston, M.H., Buffler, R.T., Shaub, F.J., McMillan, K.J., Ladd, J.W., and Worzel, J.L., 1979, Seismic evidence for widespread possible gas hydrate horizons on continental slopes and rises: American Association of Petroleum Geologists Bulletin, v. 63, p. 2204-2213

Tissot, B.T., and Welte, D.H., 1984, Petroleum formation and occurrence: New York, Springer-Verlag, 538 p.

Veevers J.J., et al., 1974, Site 262, *in* Veevers, J.J., and Heirtzler, J.R., et al., Initial Reports of the Deep Sea Drilling Project, v. 27: U.S. Government Printing Office, Washington, p. 193-278.

Veevers, J.J., 1974a, Regional site surveys, *in* Veevers, J.J., and Heirtzler, J.R., et al., Initial Reports of the Deep Sea Drilling Project, v. 27: U.S. Government Printing Office, Washington, p. 561-566.

Veevers, J.J., 1974b, Sedimentary sequences f the Timor Trough, Timor, and the Sahul Shelf, *in* Veevers, J.J., and Heirtzler, J.R., et al., Initial Reports of the Deep Sea Drilling Project, v. 27: U.S. Government Printing Office, Washington, p. 567-570.

Veevers, J.J., 1982, Western and northwestern margin of Australia, *in* Nairn, A.E.M., and Stehli, F., eds., Ocean basin and Margins: v. 6, p. 513-544.

Veevers, J.J., and Heirtzler, J.R., 1974, Tectonic and paleogeographic synthesis of Leg 27, *in* Veevers, J.J., and Heirtzler, J.R., et al., Initial Reports of the Deep Sea Drilling Project, v. 27: U.S. Government Printing Office, Washington, p. 1049-1054.

Wigley, T.M.L., Plummer, L.N., and Pearson, F.J., 1978, Mass transfer and carbon isotope evolution in natural water systems: Geochimica et Cosmochimica Acta, v. 42, p. 1117-1140.